

# Spontaneous and induced dynamic fluctuations in glass-formers I: General results and dependence on ensemble and dynamics

L. Berthier,<sup>1</sup> G. Biroli,<sup>2</sup> J.-P. Bouchaud,<sup>3,4</sup> W. Kob,<sup>1</sup> K. Miyazaki,<sup>5</sup> and D. R. Reichman<sup>5</sup>

<sup>1</sup>*Laboratoire des Colloïdes, Verres et Nanomatériaux, UMR 5587,  
Université Montpellier II and CNRS, 34095 Montpellier, France*

<sup>2</sup>*Service de Physique Théorique Orme des Merisiers – CEA Saclay, 91191 Gif sur Yvette Cedex, France*

<sup>3</sup>*Service de Physique de l’État Condensé Orme des Merisiers – CEA Saclay, 91191 Gif sur Yvette Cedex, France*

<sup>4</sup>*Science & Finance, Capital Fund Management 6-8 Bd Haussmann, 75009 Paris, France*

<sup>5</sup>*Department of Chemistry, Columbia University, 3000 Broadway, New York, NY 10027, USA*

(Dated: May 25, 2019)

We study theoretically and numerically a new family of multi-point dynamic susceptibilities that quantify the strength and characteristic lengthscales of dynamic heterogeneities in glass-forming materials. We use general theoretical arguments (fluctuation-dissipation relations and symmetries of relevant dynamical field theories) to relate the sensitivity of average two-time dynamic correlations to temperature, density, etc. to spontaneous fluctuations of the local dynamics. We discuss some subtle issues associated to the choice of microscopic dynamics and of statistical ensemble through conserved quantities (energy, density, etc.) which are found to play a major role in determining dynamic fluctuations. Our theoretical results are then compared to molecular dynamics simulations of the Newtonian, Brownian and stochastic Monte-Carlo dynamics of two representative glass-forming liquids, a fragile binary Lennard-Jones mixture and a model for the strong glass-former silica. Our main result is that dynamical correlations, in the glassy regime, are mostly driven by structural (most notably energy) fluctuations. Correspondingly, these correlations are found to be different for Newtonian dynamics (energy conserving) and for Brownian or Monte-Carlo dynamics for which energy is not conserved.

PACS numbers: 64.70.Pf, 05.20.Jj

## I. INTRODUCTION

Diverse materials, ranging from molten mixtures of metallic atoms, molecular and polymeric liquids, and colloidal suspensions may form glasses if sufficient undercooling or densification occurs [1, 2, 3]. A glass may be characterized mechanically as a solid, but microscopically lacks the long-range order of a crystal. Close to vitrification, the viscosity of glass-forming systems increases dramatically and sensitively as the thermodynamic control variables are changed. Furthermore, some degree of universality is observed in the thermal and temporal behavior of systems close to the glass transition, even though the material properties of such systems may be vastly different [1, 2]. Despite decades of intense theoretical and experimental work, the underlying causes of this interesting behavior are not well understood.

The observed quasi-universal behavior of glassy systems could be related to the existence of a growing lengthscale as the glass transition is approached. The search for such a correlation lengthscale has led to intense activity in recent years. Static structural indicators have repeatedly failed to show any evidence of collective behavior. Indeed, the static structure of a supercooled liquid hardly differs from that of the same liquid at relatively high temperatures. Clearly all simple structural correlations remain short-ranged as the glass transition is approached. It has become manifest in the last decade that interesting long-range correlations exist in spatially correlated *dynamics*. As a whole, such behavior is re-

ferred to as dynamical heterogeneity [4, 5, 6, 7, 8].

The investigation, via theory [9, 10, 11, 12, 13, 14, 15, 16], simulation [17, 18, 19, 20], and experiment [21, 22, 23, 24, 25, 26], of various aspects of dynamic heterogeneity has greatly advanced our understanding of the behavior of systems close to the glass transition. In particular, *multi-point susceptibilities* have been devised to quantify the behavior and magnitude of the putative growing dynamical lengthscale [7, 14, 15, 17, 19, 27, 28, 29, 30, 31, 32, 33], and experimental studies have, for several materials, directly determined the number of molecular units that move cooperatively near the glass transition [21, 22, 24, 25, 34, 35, 36]. Despite recent breakthroughs, much more work needs to be done to fully characterize such a behavior both experimentally and theoretically.

In the present work, contained here and in a companion paper [37], we make a step towards this goal by investigating in detail different susceptibilities that may be categorized according to the induced or spontaneous nature of the measured fluctuations [36]. Spontaneous dynamic fluctuations can be characterized by four-point functions, as proposed and studied earlier [7, 14, 15, 17, 19, 27, 28, 29, 30, 31, 32, 33]. Instead, fluctuations can be *induced* by monitoring the change of dynamical correlators that follows a change of an external control parameter (e.g. temperature). As we shall show, it is possible to relate induced and spontaneous dynamical fluctuations via fluctuation-dissipation relations as proposed in [36]. This provides a very valuable experimental tool to measure dy-

namic fluctuations since, as usual, induced fluctuations are much easier to measure than spontaneous ones.

Depending on the relevant thermodynamic ensemble and the nature of the underlying dynamics (e.g. Newtonian or Brownian), the quantitative relation between various induced and spontaneous fluctuations exhibit subtle and sometimes spectacular differences that we shall unravel both theoretically and numerically. From a theoretical point of view the comparison between induced and spontaneous fluctuations allows one to quantify how much dynamical fluctuations are driven by the structure. For instance, a question that we shall address is how much the fluctuations of dynamic correlators in super-cooled liquids are due to (short-range) energy fluctuations that, in turn, induce (long-range) dynamic fluctuations. Using molecular dynamics simulations of different archetypal glass-forming liquids (e.g. “strong” materials that exhibit an Arrhenius temperature dependence of the viscosity, and “fragile” ones, whose viscosity displays a super-Arrhenius temperature dependence) we shall show that in the slow dynamical regime a considerable fraction of spontaneous fluctuations can decisively be attributed to energy fluctuations.

Perhaps surprisingly, our analysis will also reveal that dynamical fluctuations may depend both on the statistical ensemble and on the underlying microscopic dynamics. While it is known that correlators measuring the average dynamics do not depend in the relevant glassy regime on the microscopic dynamics (Newtonian or Brownian [67]), dynamic fluctuations do so in a remarkable way. We address this problem both theoretically and numerically, and conclude that dynamical correlations depend strongly on the conserved physical quantities and on the statistical ensemble. For example, the absolute magnitude of spontaneous dynamical fluctuations in a Lennard-Jones system in the *NVT* ensemble obtained from Brownian dynamics (BD) or Monte-Carlo dynamics (MC) are quantitatively very similar, but are considerably smaller than that obtained with Newtonian dynamics (ND) in the same *NVT* ensemble, whereas simulations performed in the *NVE* ensemble yield results that are close to the BD and MC results in the *NVT* ensemble.

The aim of the present paper is to provide the reader with the physical picture underlying the dynamical susceptibilities introduced in along with more technical elements based on general field-theoretical considerations and detailed numerical investigations of different realistic glass-forming liquids.

[36], a technical analysis based on general field-theoretical considerations, and detailed numerical investigation of the relevant susceptibilities in different realistic glass-forming liquids. In a companion paper [37], we present some quantitative predictions for these susceptibilities, obtained within different theoretical models: mean-field spin glass models [38], mode-coupling theory [39], and kinetically constrained models [40] which we again confront with the results from molecular dynamics

simulations. The present paper is arranged in three sections. In Section II we present the physical motivations, definitions and physical content of several multi-point dynamic susceptibilities. We derive in particular general results for the ensemble dependence of dynamic correlations, fluctuation-dissipation relations, and bounds between induced and spontaneous dynamic fluctuations. In Section III we present a field-theoretic derivation of the behavior of dynamic fluctuations for various types of microscopic dynamics. This will be particularly useful in the discussion of the dependence of multi-point susceptibilities on the microscopic dynamics. In Section IV we present the results of detailed molecular dynamics simulations of two model glass-forming liquids, a fragile binary Lennard-Jones mixture and the strong BKS model for silica. We compare spontaneous and induced fluctuations and show that, as predicted theoretically, dynamic correlations strongly depend on the choice of microscopic dynamics and statistical ensemble.

## II. MULTI-POINT DYNAMIC CORRELATORS AND NEW LINEAR SUSCEPTIBILITIES

### A. Why four-point correlators? The spin glass case

No static correlation has yet been found to reveal any notable feature upon approaching the glass transition [41]. Any lengthscale associated with the slowing down of the system must therefore be hidden in some dynamic correlation function. This issue is in fact deeply related to one of the most important question pertaining to the physics of disordered systems – how can one define *long-range amorphous order* in such systems?

We know from the theory of spin glasses that the above oxymoron has in fact a precise answer: some hidden long-range order indeed develops at the spin glass transition [42]. In order to reveal this long-range order, conventional two-point functions are useless. Even if spins  $s_x$  and  $s_{x+y}$  have non-zero static correlations  $\langle s_x s_{x+y} \rangle$  in the spin glass phase, the average over space for a given distance  $y$  vanishes because the pairwise correlations randomly change sign whenever  $x$  changes. The insight of Edwards and Anderson is that one should first square  $\langle s_x s_{x+y} \rangle$  before averaging over space [43]. In this case, the resulting (four-spin) correlation function indeed develops long-range tails in the spin glass phase. This correlation in fact decays so slowly that its volume integral, related to the non-linear magnetic susceptibility of the material, diverges in the whole spin glass phase, see e.g. [44].

The Edwards-Anderson idea can in fact be understood from a dynamical point of view, which is important for understanding both the physics of the spin glass just above the transition, and its generalization to structural glasses. Consider, in the language of spins, the following four-point correlation function:

$$G_4(\mathbf{y}, t) = [\langle s_x(t=0) s_{x+y}(t=0) s_x(t) s_{x+y}(t) \rangle]_x, \quad (1)$$

where the brackets  $[...]_x$  indicate a spatial average. Suppose that spins  $s_{\mathbf{x}}$  and  $s_{\mathbf{x}+\mathbf{y}}$  develop static correlations  $\langle s_{\mathbf{x}} s_{\mathbf{x}+\mathbf{y}} \rangle$  within the glass phase. In this case,  $G_4(\mathbf{y}, t \rightarrow \infty)$  will clearly converge to the spin glass correlation  $[\langle s_{\mathbf{x}} s_{\mathbf{x}+\mathbf{y}} \rangle^2]_x$ . More generally,  $G_4(\mathbf{y}, t)$  for finite  $t$  is able to detect *transient* tendencies to spin glass order, for example slightly above the spin glass transition temperature  $T_c$ . Close to the spin glass transition, both the persistence time and the dynamic length diverge in a critical way:

$$G_4(\mathbf{y}, t) \approx y^{2-d-\eta} \hat{G} \left( \frac{y}{\xi}, \frac{t}{\tau} \right), \quad (2)$$

where  $\xi \sim (T - T_c)^{-\nu}$  and  $\tau \sim (T - T_c)^{-z\nu}$ . As mentioned above, the static non-linear susceptibility diverges as  $\int d\mathbf{y} G_4(\mathbf{y}, t \rightarrow \infty) \sim \xi^{2-\eta}$ . More generally, one can define a time-dependent dynamic susceptibility as:

$$\chi_4(t) \equiv \int d\mathbf{y} G_4(\mathbf{y}, t), \quad (3)$$

which defines a correlation volume, i.e. the typical number of spins correlated in dynamic events taking place over the time scale  $t$ . As we shall discuss below,  $\chi_4(t)$  can also be interpreted as a quantitative measure of the dynamic fluctuations. Note however that the precise relation between  $\chi_4$  and  $\xi$  depends on the value of the exponent  $\eta$ , which is physically controlled by the detailed spatial structure of  $G_4$ :

$$\chi_4(t = \tau) \propto \xi^{2-\eta}. \quad (4)$$

Therefore, spin glasses offer a precise example of a system which gets slower and slower upon approaching  $T_c$  but without any detectable long-range order appearing in two-point correlation functions. Only more complicated four-point functions are sensitive to the genuine amorphous long-range order that sets in at  $T_c$  and give non-trivial information even above  $T_c$ . In the case of spin glasses it is well established that the transition is related to the emergence of a low temperature thermodynamic phase characterized by amorphous long-range order. In the case of the glass transition of viscous liquids the situation is much less clear. There might be no true phase transition toward a low temperature amorphous phase. It is still reasonable to expect that the dramatic increase of the relaxation time is due to a transient amorphous order that sets in and whose range grows approaching the glass transition. Growing timescales should be somehow related to growing lengthscales [45]. A good candidate to unveil the existence of this phenomenon is the function  $G_4(\mathbf{y}, t)$  introduced previously, since nothing in the above arguments was specific to systems with quenched disorder. The only difference is that although transient order is detected in  $G_4(\mathbf{y}, t)$  or its volume integral  $\chi_4(t)$  for times of the order of the relaxation time, in the long time limit these two functions may not, and indeed do not in the case of supercooled liquids, show long-range amorphous order. This roots back to the different nature

of the glass and spin glass transitions (see the discussion in [44]).

## B. Supercooled liquids and more multi-point correlations

In the case of liquids, we may consider a certain space dependent observable  $o(\mathbf{x}, t)$ , such as, for example, the local excess density  $\delta\rho(\mathbf{x}, t) = \rho(\mathbf{x}, t) - \rho_0$ , where  $\rho_0$  is the average density of the liquid, or the local dipole moment, the excess energy, etc. We will assume in the following that the average of  $o(\mathbf{x}, t)$  is equal to zero, and the variance of  $o(\mathbf{x}, t)$  normalized to unity. The dynamic two-point correlation is defined as:

$$C_o(\mathbf{r}, t) = [o(\mathbf{x}, t = 0)o(\mathbf{x} + \mathbf{r}, t)]_x, \quad (5)$$

where the normalization ensures that  $C_o(\mathbf{r} = \mathbf{0}, t = 0) = 1$ . The Fourier transform of  $C_o(\mathbf{r}, t)$  defines a generalized dynamic structure factor  $S_o(\mathbf{k}, t)$  [46]. All experimental and numerical results known to date suggest that as the glass transition is approached, no spatial anomaly of any kind appears in  $C_o(\mathbf{r}, t)$  (or in  $S_o(\mathbf{k}, t)$ ) although of course there could still be some signal which is perhaps too small to be measurable. The only remarkable feature is that the slowing down of the two-point correlation functions often obeys, to a good approximation, “time-temperature superposition” in the  $\alpha$ -relaxation regime, i.e.:

$$C_o(\mathbf{r}, t) \approx q_o(\mathbf{r}) f \left( \frac{t}{\tau_\alpha(T)} \right), \quad (6)$$

where  $q_o$  is often called the non-ergodicity (or Edwards-Anderson) parameter, and the scaling function  $f(x)$  depends only weakly on temperature. This property will be used to simplify the following discussions, but it is not a crucial ingredient.

Whereas  $C_o(\mathbf{r}, t)$  measures how, on average, the dynamics decorrelates the observable  $o(\mathbf{x}, t)$ , it is natural to ask whether this decorrelation process is homogeneous in space and in time. Can the correlation last much longer than average? In other words, what is the distribution (over possible dynamical histories) of the correlation  $C_o(\mathbf{r}, t)$ ? Clearly, since  $C_o(\mathbf{r}, t)$  is defined as an average over some large volume  $V$ , the variance  $\Sigma_C^2$  of  $C_o(\mathbf{r}, t)$  is expected to be of order  $1/V$ . More precisely we define:

$$\begin{aligned} \Sigma_C^2 = & \int \frac{d\mathbf{x}}{V} \frac{d\mathbf{x}'}{V} o(\mathbf{x}, 0)o(\mathbf{x} + \mathbf{r}, t)o(\mathbf{x}', 0)o(\mathbf{x}' + \mathbf{r}, t) \\ & - C_o(\mathbf{r}, t)^2, \end{aligned} \quad (7)$$

which, using translational invariance, can be transformed into the space integral of a four-point correlation:

$$\Sigma_C^2 = \int \frac{d\mathbf{y}}{V} G_4(\mathbf{y}, t), \quad (8)$$

where

$$G_4(\mathbf{y}, t) = \left\{ [o(\mathbf{x}, 0)o(\mathbf{x} + \mathbf{r}, t)o(\mathbf{x} + \mathbf{y}, 0)o(\mathbf{x} + \mathbf{y} + \mathbf{r}, t)]_x - [o(\mathbf{x}, t = 0)o(\mathbf{x} + \mathbf{r}, t)]_x^2 \right\}. \quad (9)$$

The variance of  $C_o(\mathbf{r}, t)$  can thus be expressed as an integral over space of a four-point correlation function, which measures the spatial correlation of the temporal correlation. This integral over space is also the Fourier transform of  $G_4(\mathbf{y}, t)$  with respect to  $\mathbf{y}$  at the wavevector  $\mathbf{q}$  equal to zero. We want to insist at this stage that  $\mathbf{r}$  and  $\mathbf{y}$  in the above equations play very different roles: the former enters the very definition of the correlator we are interested in Eq. (5), whereas the latter is associated with the scale over which the dynamics is potentially correlated. Correspondingly, great care will be devoted in the following to distinguish the wavevector  $\mathbf{k}$ , conjugate to  $\mathbf{r}$ , and  $\mathbf{q}$  conjugate to  $\mathbf{y}$ .

Specializing to the case  $\mathbf{r} = 0$  (local dynamics), one finally obtains [79]:

$$\Sigma_C^2 \equiv \frac{\chi_4(t)}{N}. \quad (10)$$

The analogy with spin glasses developed above suggests that this quantity reveals the emergence of amorphous long-range order; it is in fact the natural diverging susceptibility in the context of  $p$ -spin descriptions of supercooled liquids, where a true dynamical phase transition occurs at a certain critical temperature [16, 27, 47, 48]. Since in real systems no true phase transition is observed, one expects  $\chi_4(t)$  to grow until  $t \approx \tau_\alpha$  and decay back to zero thereafter. Until  $\tau_\alpha$ , there cannot be strong differences between a system with quenched disorder and a system where disorder is dynamically self-induced.

In practice,  $\chi_4(t)$  is not computed from the fluctuations of  $C_o(\mathbf{0}, t)$ . Contrary to spin glasses, for which an underlying lattice structure exists, viscous liquids consist of molecules or atoms having continuum positions. As a consequence, one has to coarse-grain space in order to measure the fluctuations of the local relaxation dynamics. Local now means on a region of the order of the interparticle distance. Therefore, generically,  $\chi_4(t) = V\Sigma_C^2$  correspond either to the fluctuations of the Fourier transform of  $C_o(\mathbf{r}, t)$  evaluated at a wave-vector,  $k_0$ , of the order of the first peak in the structure factor [32], or to a spatial average  $\int d\mathbf{r} C_o(\mathbf{r}, t)w(\mathbf{r})$  where  $w(\mathbf{r})$  is an overlap function equal to one for lengths of the order of  $2\pi/k_0$  and zero otherwise [7]. The dependence of dynamical correlations on the coarse-graining length has been recently studied in [49] and is also discussed in the companion paper [37].

Although readily accessible in numerical simulations,  $\Sigma_C^2$  is in general very small and impossible to measure directly in experiments, except when the range of the dynamic correlation is macroscopic, as in granular materials [35] or in soft glassy materials where it can reach the micrometer and even millimeter range [34, 50].

The central idea of this work is that induced dynamic fluctuations are more accessible than spontaneous ones, and can be related to one another by fluctuation-dissipation theorems. The physical motivation is that while four-point correlations offer a direct probe of the dynamic heterogeneities, other multi-point correlation functions give very useful information about the microscopic mechanisms leading to these heterogeneities. For example, one expects that a local positive energy fluctuation per unit volume  $\delta e$  (or a negative density fluctuation) at  $\mathbf{x}$  and time  $t = 0$  triggers or eases the dynamics in its surroundings, leading to a systematic correlation between  $\delta e(\mathbf{x}, t = 0)$  and  $o(\mathbf{x}', t = 0)o(\mathbf{x}' + \mathbf{r}, t)$ . This defines a family of three-point correlation functions that relate thermodynamic or structural fluctuations to dynamics. As we discuss now, some of these three-point correlations are both experimentally accessible and give bounds or approximations to the four-point dynamic correlations. The reason is as follows. In the same way that the space integral of the four-point correlation function is the variance of the two-point correlation, the space integral of the above three-point correlation is the covariance of the dynamic correlation with the energy fluctuations [80]:

$$\Sigma_{CE} = \frac{1}{VN} \int d\mathbf{x} d\mathbf{x}' o(\mathbf{x}' + \mathbf{r}, t)o(\mathbf{x}', 0)\delta e(\mathbf{x}, 0) \equiv \frac{1}{N} \int d\mathbf{y} [o(\mathbf{x} + \mathbf{y} + \mathbf{r}, t)o(\mathbf{x} + \mathbf{y}, 0)\delta e(\mathbf{x}, 0)]_x. \quad (11)$$

Hence, using the fact that the energy fluctuations per particle are of order  $\sqrt{c_V k_B T}$  (where  $c_V$  is the specific heat in  $k_B$  units), the quantity  $N\Sigma_{CE}/\sqrt{c_V k_B T}$  defines the *number of particles* over which energy and dynamics are correlated. Of course, analogous identities can be derived for the covariance with density fluctuations.

Now, on very general grounds, the covariance obeys the following Cauchy-Schwarz bound:  $\Sigma_{CE}^2 \leq \Sigma_C^2 \Sigma_E^2$ , where  $\Sigma_E$  is the variance of the energy fluctuations, equal to  $c_V(k_B T)^2/N$  in the  $NVT$  ensemble,  $N = \rho_0 V$  being the total number of particles. Therefore, the dynamic susceptibility  $\chi_4(t)$  is bounded from below by:

$$\chi_4(t) \equiv N\Sigma_C^2 \geq \frac{N^2 \Sigma_{CE}^2}{N\Sigma_E^2} = \left( \frac{N\Sigma_{CE}}{\sqrt{c_V(k_B T)}} \right)^2, \quad (12)$$

where, as we show below, the right hand side is easily accessible experimentally. We then discuss in Sec. II E how the above bound can be interpreted as an approximation, with corrections that can be physically estimated. Note that we chose here to define  $\chi_4(t)$  as a number of particles; one can of course convert it into a volume by multiplying  $\chi_4$  by  $v_0 = 1/\rho_0$ , the average volume per particle. Note also that here and in the following we will work in the  $NVT$  ensemble. We will discuss later the generalization to different ensembles.

### C. A dynamic fluctuation-dissipation theorem and growing lengthscales

Consider a system in the canonical  $NVT$  ensemble. The probability of a given configuration  $\mathcal{C}$  is well known to be given by the Boltzmann weight  $\exp(-\beta E[\mathcal{C}])/Z$ , where  $\beta = 1/k_B T$ . Suppose one studies an observable  $O$  with the following properties: (i)  $O$  only depends on the current microscopic configuration  $\mathcal{C}$  of the system and (ii)  $O$  can be written as a sum of local contributions:

$$O = \frac{1}{V} \int d\mathbf{x} o(\mathbf{x}). \quad (13)$$

In this case, a well-known static fluctuation-dissipation theorem holds [46]:

$$\frac{\partial \langle O \rangle}{\partial \beta} = - \int d\mathbf{x} \langle o(\mathbf{x}) \delta e(\mathbf{0}) \rangle \equiv -N \Sigma_{OE}, \quad (14)$$

where we assumed that the energy can be written as a sum of local contributions.

Interestingly, in the case of *deterministic* Hamiltonian dynamics, the value of any local observable  $o(\mathbf{x}, t)$  is in fact a highly complicated function of the initial configuration at time  $t = 0$ . Therefore, the correlation function, now averaged over both space and initial conditions can be written as a thermodynamical average:

$$C_o(\mathbf{r}, t; T) = \frac{1}{Z(\beta)V} \int d\mathbf{x} o(\mathbf{x} + \mathbf{r}, t) o(\mathbf{x}, t = 0) \times \exp \left[ -\beta \int d\mathbf{x}' e(\mathbf{x}', t = 0) \right]. \quad (15)$$

Hence, the derivative of the correlation with respect to temperature directly leads, in the case of purely conservative Hamiltonian dynamics, to the covariance between initial energy fluctuations and the following dynamical correlation:

$$\frac{\partial C_o(\mathbf{r}, t; T)}{\partial T} = \frac{1}{k_B T^2} \int d\mathbf{x} \langle o(\mathbf{x} + \mathbf{r}, t) o(\mathbf{x}, 0) \delta e(\mathbf{0}, 0) \rangle \equiv \chi_T(\mathbf{r}, t). \quad (16)$$

Hence, the sensitivity of the dynamics to temperature is directly related to a dynamic correlation. This equality, although in a sense trivial, is one of the central result of this work, and has an immediate deep physical consequence, which is the *growth of a dynamical length upon cooling in glassy systems*. Define  $\tau_\alpha(T)$  such that  $C_o(\mathbf{0}, t = \tau_\alpha; T) = e^{-1}$  (say). Differentiating this definition with respect to  $T$  gives

$$0 = \frac{d\tau_\alpha}{dT} \frac{\partial C_o(\mathbf{0}, t = \tau_\alpha; T)}{\partial t} + \frac{\partial C_o(\mathbf{0}, t = \tau_\alpha; T)}{\partial T}. \quad (17)$$

Since  $C_o(\mathbf{0}, t; T)$  decays from 1 to zero over a time scale  $\tau_\alpha$ , one finds that generically, using Eq. (16):

$$\int d\mathbf{x} \langle o(\mathbf{x}, t = \tau_\alpha) o(\mathbf{x}, 0) \delta e(\mathbf{0}, 0) \rangle \sim k_B T \frac{d \ln \tau_\alpha}{d \ln T}. \quad (18)$$

But since  $\delta e$  is of order  $\rho_0 \sqrt{c_V k_B T}$  and  $\langle o^2 \rangle$  is normalized to unity, an increase of the right hand side of the equality (16) necessarily implies the growth of the volume  $\chi_T$  over which energy fluctuations and dynamics are correlated. More precisely, as soon as  $\tau_\alpha$  increases faster than any inverse power of temperature, the slowing down of a Hamiltonian system is necessarily accompanied by the growth of a dynamic correlation length. However, as already mentioned above, the precise relation between the volume defined by  $\chi_T$  and an actual *lengthscale*,  $\xi_T$ , depends on the detailed structure of the spatial correlation function (for example the value of the exponent  $\eta$ ).

It is instructive to study in detail the case of a strong glass-former, for which the slowing down is purely Arrhenius, i.e.  $\tau_\alpha = \tau_0 \exp[\Delta/(k_B T)]$ , where  $\Delta$  is some activation barrier. The volume  $\chi_T$  is then given by:

$$|\chi_T(\tau_\alpha)| \sim \frac{d \ln \tau_\alpha}{d \ln T} = \frac{\Delta}{k_B T}, \quad (19)$$

which increases as the temperature is decreased. This is at first sight contrary to intuition since simple barrier activation seems to be a purely local process. However, one should remember that the dynamics strictly conserves energy, so that the energy used to cross a barrier must flow from other parts of the system. Hence, even in a strong glass, the seemingly trivial Arrhenius slowing down is necessarily accompanied by the growth of a dynamic lengthscale.

When the relaxation time diverges in a Vogel-Fulcher manner, i.e.  $\tau_\alpha = \tau_0 \exp[DT_0/(T - T_0)]$ , one finds that the corresponding dynamic correlation volume also diverges at  $T_0$ , as:

$$\chi_T(\tau_\alpha) \sim \frac{DT_0}{(T - T_0)^2} \propto (\ln \tau_\alpha)^2, \quad (20)$$

where the last estimate holds sufficiently close to  $T_0$ .

More generally, one can study the behavior of  $\chi_T(\mathbf{0}, t) \sim \partial C_o(\mathbf{0}, t; T) / \partial T$  as a function of time. Since at all temperature  $C_o(\mathbf{0}, t = 0; T) = 1$  and  $C_o(\mathbf{0}, \infty; T) = 0$ , it is clear that  $\chi_T(\mathbf{0}, t)$  is zero at short and long times. We illustrate in Fig. 1 the shape of  $\chi_T(\mathbf{0}, t)$  for two glass-formers studied by molecular dynamics simulations described in Sec. IV. It has a peak for  $t \approx \tau_\alpha$ . It is useful to keep in mind the example where the correlation function is a stretched exponential with exponent  $\beta$  [not to be confused with  $1/k_B T$ ], in which case:

$$\frac{\partial C_o(\mathbf{0}, t; T)}{\partial \ln T} = \frac{d \ln \tau_\alpha}{d \ln T} \beta \left( \frac{t}{\tau_\alpha} \right)^\beta \exp \left[ - \left( \frac{t}{\tau_\alpha} \right)^\beta \right]. \quad (21)$$

It is easy to show that this function behaves as a power-law,  $t^\beta$ , at small times and reaches a maximum for  $t = \tau_\alpha$ ; before decaying to zero. The power-law at small times appears in the context of many different models, as also discussed for the time behavior of  $\chi_4(t)$  [33]. Note also that for  $t = \tau_\alpha$  and  $T = T_g$ , one has:

$$\left. \frac{\partial C_o(\mathbf{0}, \tau_\alpha; T)}{\partial \ln T} \right|_{T_g} = \beta m \ln 10, \quad (22)$$

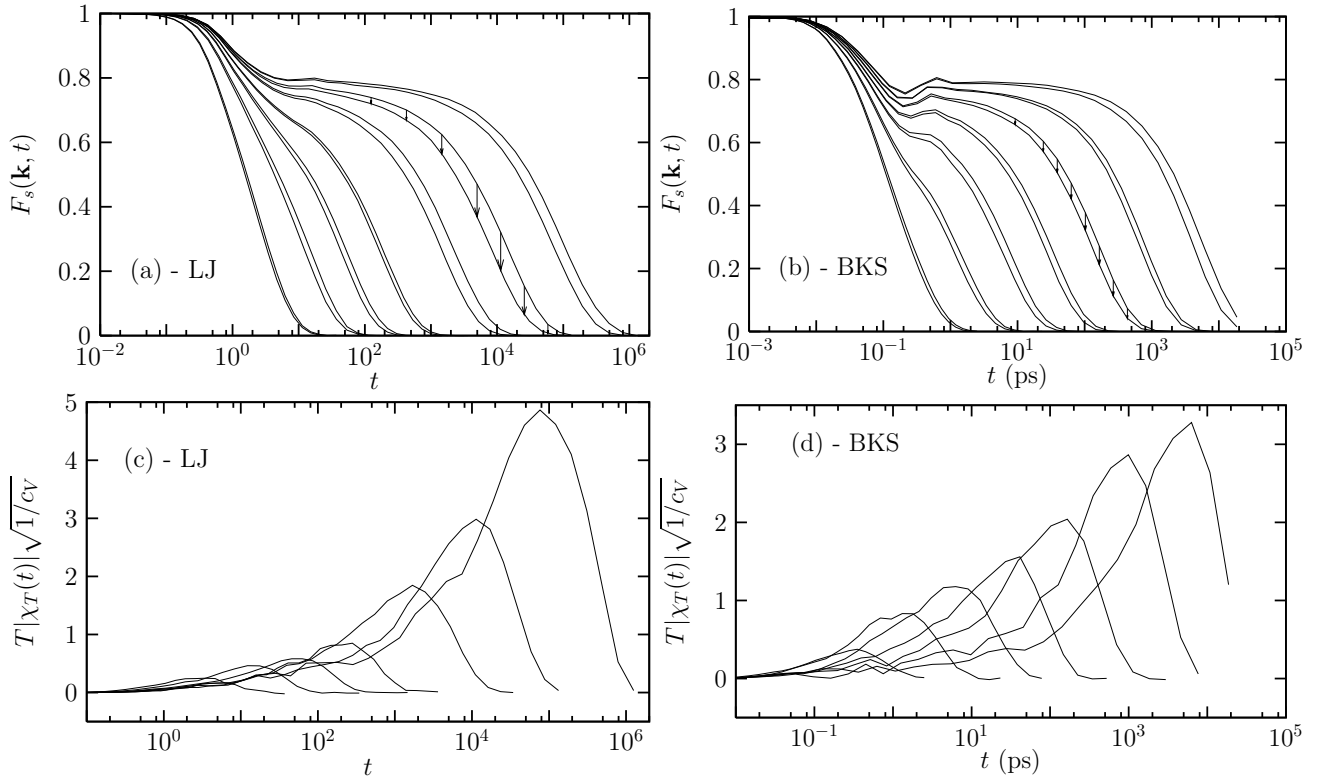


FIG. 1: (a) and (b) respectively show the self-intermediate scattering functions  $F_s(\mathbf{k}, t)$  as a function of time for various temperatures in a binary Lennard-Jones mixture and the BKS model for silica, obtained from the molecular dynamics numerical simulations discussed in Sec. IV. (a)  $T = 2.1, 2.0, 1.05, 1.0, 0.75, 0.72, 0.61, 0.6, 0.51, 0.5, 0.47, 0.46, 0.435$  and  $0.43$  from left to right. (b)  $T = 6100, 5900, 4700, 4600, 4000, 3920, 3580, 3520, 3250, 3200, 3000, 2960, 2750$ , and  $2715$  K from left to right. The arrows illustrate how  $\chi_T = \partial F_s / \partial T$  is obtained by finite difference for each couple of temperatures. (c) and (d) show the resulting  $\chi_T(t)$  for both models, normalized by the strength of energy fluctuations. We show the absolute value since  $\chi_T$  is a negative quantity. In both liquids the dynamic susceptibility presents a peak for  $t \approx \tau_\alpha$  whose height increases as temperature decreases, revealing increasingly heterogeneous and spatially correlated dynamics.

where  $m = T d \log_{10} \tau_\alpha / dT|_{T_g}$  is the steepness index, which characterizes the fragility of the glass. Note that in many cases, the resulting numerical value of  $\chi_T$  turns out to be already large in the late  $\beta$ -regime, meaning that the concept of a cage is misleading because caging in fact involves the correlated motion of many particles [35, 48].

Using the inequality in Eq. (12) with the results of the present section, we finally obtain a lower bound on  $\chi_4(t)$  for Newtonian systems which is experimentally accessible:

$$\chi_4(\mathbf{r}, t) \geq \frac{T^2 \chi_T(\mathbf{r}, t)^2}{c_V} = \frac{1}{c_V} \left( \frac{\partial C_o(\mathbf{r}, t; T)}{\partial \ln T} \right)^2. \quad (23)$$

In the case of Arrhenius dynamics, the volume defined by the lower bound is given by  $\Delta^2 / (k_B c_V T^2)$ . Physically, this is the smallest volume for which typical thermodynamic fluctuations of the energy are equal to the energy barrier  $\Delta$ . For a Vogel-Fulcher divergence, one now finds the bounds to be proportional to  $(\ln \tau_\alpha)^4$ .

The above result in Eq. (23) is extremely general and applies to different situations discussed in the next section. It however does *not* apply when the dynam-

ics is not Newtonian, as would be the case for Brownian particles, for example, or, in numerical simulations, when one uses Monte-Carlo dynamics [51, 52]. The reason is that in these cases, not only the initial probability but also the transition probability from the initial to the final configuration itself explicitly depends on temperature. In Brownian dynamics, for example, the noise in the Langevin equation depends on temperature. Hence,  $\partial C_o(\mathbf{r}, t; T) / \partial T$  receives extra contributions from the whole trajectory, that depend on the explicit choice of dynamics. We will see below that when a dynamical critical point exists or is narrowly avoided, a system with Brownian dynamics displays dynamical correlations of the form  $\chi_4 \sim \chi_T$  rather than the scaling  $\chi_4 \sim \chi_T^2$  suggested by the above bound, Eq. (23).

## D. Several generalizations

### 1. Enthalpy rather than energy

The above results were obtained within the *NVT* ensemble, where energy fluctuations are relevant. In many applications, however, pressure rather than volume is held fixed. In this fixed pressure ensemble, the probability of a given configuration is given by:

$$P(\mathcal{C}) = \frac{1}{Z} \exp \left[ -\beta \int d\mathbf{x} h(\mathbf{x}) \right], \quad (24)$$

where  $h = e + \rho_0 Pv$  is the enthalpy density of the fluid,  $P$  is the pressure and  $v$  the local volume per particle. Since the variance of enthalpy fluctuations per particle is equal to  $N\Sigma_H^2 = c_P k_B T^2$ , all the above results carry through with  $c_V$  replaced by  $c_P$ , in particular:

$$\chi_4(\mathbf{r}, t) \geq \frac{1}{c_P} \left( \frac{\partial C_o(\mathbf{r}, t; T)}{\partial \ln T} \right)^2. \quad (25)$$

### 2. Density rather than temperature

In the above section, we have shown that the response of the correlator to a change of temperature is related to dynamic correlations. Other perturbing fields may also be relevant, such as density, pressure, concentration of species in the case of mixtures, etc. For example, for hard-sphere colloids, temperature plays very little role whereas small changes of density can lead to enormous changes in relaxation times [53]. Using Eq. (24) for the probability of initial configurations in the *NPT* ensemble, and the fact that the dynamics only depends on the initial condition, one now derives the following equality:

$$\frac{\partial C_o(\mathbf{r}, t; P)}{\partial P} \Big|_T = -\frac{\rho_0}{k_B T} \int d\mathbf{x} \langle o(\mathbf{x} + \mathbf{r}, t) o(\mathbf{x}, 0) \delta v(\mathbf{0}, 0) \rangle, \quad (26)$$

which can again be used to define a dynamic correlation volume  $\chi_\rho$ . Introducing the isothermal compressibility  $\kappa_T = (\partial \rho / \partial P)|_T / \rho_0$  and noting that the total variance of volume fluctuations per particle is given by  $k_B T \kappa_T / \rho_0$ , we find:

$$\begin{aligned} N\Sigma_{CV} &= \rho_0 \int d\mathbf{x} \langle o(\mathbf{x} + \mathbf{r}, t) o(\mathbf{x}, t=0) \delta v(\mathbf{0}, t=0) \rangle \\ &= -k_B T \kappa_T \frac{\partial C_o(\mathbf{r}, t; \rho)}{\partial \ln \rho} \Big|_T, \end{aligned} \quad (27)$$

from which we deduce a second bound on the dynamic correlation volume  $\chi_4(t)$ :

$$\chi_4(\mathbf{r}, t) \geq \rho_0 k_B T \kappa_T \left( \frac{\partial C_o(\mathbf{r}, t; \rho)}{\partial \ln \rho} \right)^2. \quad (28)$$

Again, the right hand side of this expression is accessible to experiments [36]. Very importantly, and contrarily

to the case of temperature, this inequality holds even for Brownian dynamics since the statistics of trajectories has no explicit dependence on pressure or density. Finally, a similar inequality holds for binary mixtures, relating  $\chi_4(t)$  to the dependence of the correlation function on the mixture composition.

### 3. Correlation and response in frequency space

We have considered up to now the variance of the correlation function for a given time  $t$ , related to the four-point susceptibility  $\chi_4(t)$ , but this can be generalized to the covariance of the correlation at two different times  $t$  and  $t'$ , defined as:

$$\begin{aligned} \Xi_4(\mathbf{r}; t, t') &\equiv \int \frac{d\mathbf{x}}{V} \frac{d\mathbf{x}'}{V} o(\mathbf{x}, 0) o(\mathbf{x} + \mathbf{r}, t) o(\mathbf{x}', 0) o(\mathbf{x}' + \mathbf{r}, t') \\ &\quad - C_o(\mathbf{r}, t) C_o(\mathbf{r}, t'), \end{aligned} \quad (29)$$

with  $\Xi_4(\mathbf{r}; t, t) = \chi_4(\mathbf{r}, t)$ . Using the Cauchy-Schwarz inequality  $\langle (A + B)C \rangle^2 / \langle C^2 \rangle - \langle A^2 + B^2 \rangle \leq 2 \langle AB \rangle$  one can again establish a lower bound for this quantity, which reads, in the *NVT* ensemble:

$$\begin{aligned} \Xi_4(\mathbf{r}; t, t') &\geq \frac{1}{2c_V} \left[ \left( \frac{\partial C_o(\mathbf{r}, t; T)}{\partial \ln T} \right) + \left( \frac{\partial C_o(\mathbf{r}, t'; T)}{\partial \ln T} \right) \right]^2 \\ &\quad - \frac{1}{2} [\chi_4(\mathbf{r}, t) + \chi_4(\mathbf{r}, t')]. \end{aligned} \quad (30)$$

It is useful to translate this result into Fourier space. Defining  $C_o(\mathbf{r}, \omega) = \int dt e^{i\omega t} C_o(\mathbf{r}, t)$ , the fluctuations of  $C_o(\mathbf{r}, \omega)$  define a four-point susceptibility in Fourier space  $\chi_4(\mathbf{r}, \omega)$  given by:

$$\chi_4(\mathbf{r}, \omega) = \int dt dt' e^{i\omega(t+t')} \Xi_4(\mathbf{r}; t, t'). \quad (31)$$

Using the above upper bound, Eq. (30), one finds, whenever  $\omega \neq 0$ :

$$\chi_4(\mathbf{r}, \omega) \geq \frac{1}{c_V} \left( \frac{\partial C_o(\mathbf{r}, \omega; T)}{\partial \ln T} \right)^2. \quad (32)$$

We have up to now considered correlation functions, but the very same string of arguments also applies to linear response functions, which can, in the context of Newtonian dynamics, be written solely as functions of the initial condition. For example, the susceptibility of the observable  $o$  to an external field  $X$  is:

$$\begin{aligned} \chi_o(\mathbf{r}, t) &= \frac{1}{Z(\beta)V} \int d\mathbf{x} \frac{\delta o(\mathbf{x} + \mathbf{r}, t)}{\delta X(\mathbf{x}, t=0)} \times \\ &\quad \exp \left[ -\beta \int d\mathbf{x}' e(\mathbf{x}', t=0) \right], \end{aligned} \quad (33)$$

from which all the above results, transposed to response functions, can be derived. This is an important remark, since response functions, such as frequency dependent dielectric response or elastic moduli, are routinely measured in glassy materials. Their temperature or density dependence is therefore a direct probe of the dynamic correlation in these materials [36].

#### 4. Higher derivatives

One can of course study higher derivatives of the correlation functions with respect to temperature, which lead to higher order multi-point correlations between dynamics and energy or density fluctuations. For example, the second derivative gives a connected four-point correlation function:

$$\frac{\partial^2 C_o(\mathbf{0}, t; T)}{\partial \beta^2} = \int d\mathbf{x} d\mathbf{y} \langle o(\mathbf{x}, t) o(\mathbf{x}, 0) \delta e(\mathbf{y}, 0) \delta e(\mathbf{0}, 0) \rangle_c. \quad (34)$$

The right hand side now defines a squared correlation volume, where the left hand side, computed for  $t = \tau_\alpha$ , contains terms proportional to  $d^2 \ln \tau_\alpha / d \ln T^2$  and to  $(d \ln \tau_\alpha / d \ln T)^2$ . In most cases where  $\ln \tau_\alpha$  diverges as an inverse power of temperature, or in a Vogel-Fulcher-like manner, one finds that the latter term dominates over the former. This means that this squared correlation volume in fact behaves like  $\chi_T^2$ . The same argument also holds for higher derivatives.

### E. Fluctuations and ensembles

#### 1. Constrained vs. unconstrained fluctuations

The above upper bounds in Eqs. (23, 25) can in fact be given a much more precise meaning by realizing that fluctuations of thermodynamic quantities are Gaussian in the large volume limit [54], except at a critical point. This allows one to show the following general result. Consider an observable  $O$  that depends on  $M$  Gaussian random variables  $z_1, z_2, \dots, z_M$ . We want to compare the ensemble where all the  $z_i$ 's are free to fluctuate with the ensemble where one constrains a subset of the  $z_i$ , say  $z_m, \dots, z_M$  to take fixed values, with no fluctuations. In the limit of small fluctuations, the variances of  $O$  in the two ensembles are related through:

$$\Sigma_O^2 = \langle O^2 | z_m, \dots, z_M \rangle_c + \sum_{\alpha, \beta=m}^M \frac{\partial \langle O | z_m, \dots, z_M \rangle}{\partial z_\alpha} \frac{\partial \langle O | z_m, \dots, z_M \rangle}{\partial z_\beta} \langle z_\alpha z_\beta \rangle_c, \quad (35)$$

where the average in the ensemble where  $z_m, \dots, z_M$  are fixed is denoted by  $\langle \cdot | z_m, \dots, z_M \rangle$ . The subscript  $c$  means that we consider connected averages and we use Greek indices for the  $(M - m + 1)$  constrained variables.

Because this result is important throughout this paper, we sketch here its proof, using ideas and a notation which should make clear the analogy with a similar result derived in Sec. III using a field theoretical representation for the dynamics of supercooled liquids. Without loss of generality, we can choose the mean of all  $z_i$ 's to be zero. The unconstrained joint distribution of the  $z_i$ 's can be

written as:

$$P(\{z_i\}) = \frac{\sqrt{\det D}}{(2\pi)^{M/2}} \exp \left( -\frac{1}{2} \sum_{ij} z_i D_{ij} z_j \right), \quad (36)$$

where  $D$  is a certain  $M \times M$  symmetric positive definite matrix. The unconstrained covariance between  $z_i$  and  $z_j$  is well-known to be given by:

$$\langle z_i z_j \rangle = (D^{-1})_{ij}. \quad (37)$$

Let us now write  $D$  as blocks corresponding to the  $(m-1)$  fluctuating variables and the  $(M-m+1)$  fixed variables:

$$D = \begin{bmatrix} A & B \\ B^\dagger & C \end{bmatrix}, \quad (38)$$

where  $A$  is  $(m-1) \times (m-1)$ ,  $B$  is  $(m-1) \times (M-m+1)$  and  $C$  is  $(M-m+1) \times (M-m+1)$ . When the variables  $z_m, \dots, z_M$  are fixed, the unconstrained variables acquire non-zero average values which are easily found to be given by:

$$\bar{z}_i = \sum_{\alpha=m}^M (A^{-1} B)_{i\alpha} z_\alpha. \quad (39)$$

To establish the relation between constrained and unconstrained covariances, we note the following block matrix inversion rule:

$$D^{-1} = \begin{bmatrix} \{A - BC^{-1}B^\dagger\}^{-1} & -\{CB^{-1}A - B^\dagger\}^{-1} \\ -\{A(B^\dagger)^{-1}C - B\}^{-1} & \{C - B^\dagger A^{-1}B\}^{-1} \end{bmatrix}, \quad (40)$$

together with the matrix identity:

$$\{A - BC^{-1}B^\dagger\}^{-1} = A^{-1} + (A^{-1}B)\{C - B^\dagger A^{-1}B\}^{-1}(A^{-1}B)^\dagger. \quad (41)$$

The constrained covariance  $\langle z_i z_j | z_m, \dots, z_M \rangle_c$  is clearly given by  $(A^{-1})_{ij}$ . Using the above identities, we directly obtain:

$$\langle z_i z_j \rangle \equiv \langle z_i z_j | z_m, \dots, z_M \rangle_c + \sum_{\alpha, \beta} \frac{\partial \bar{z}_i}{\partial z_\alpha} \frac{\partial \bar{z}_j}{\partial z_\beta} \langle z_\alpha z_\beta \rangle. \quad (42)$$

Now, the final result Eq. (35) above can be established simply by considering, to lowest order in the fluctuations, the observable  $O$  as an  $M+1$ th Gaussian variable correlated with all the  $z_i$ 's and apply the above equality to  $i = j = M+1$ .

#### 2. From NVE to NVT

Let us apply the general result Eq. (35) to the case of interest here, first to the case  $M = 1$ , with  $z_1 = E$  and number of particles and volume fixed. The two ensembles correspond to  $NVT$  and  $NVE$ , respectively. The

above formula can be used with the correlation  $C_o$  as an observable provided the dynamics is conservative, as argued above. Therefore:

$$\chi_4^{NVT}(\mathbf{r}, t) = \chi_4^{NVE}(\mathbf{r}, t) + \frac{1}{c_V} \left( \frac{\partial C_o(\mathbf{r}, t; T)}{\partial \ln T} \right)^2, \quad (43)$$

where we have replaced in the second term in the right hand side  $\partial/\partial E$  by  $(1/Nc_V k_B)\partial/\partial T$ ;  $\chi_4^{NVE}(\mathbf{r}, t)$  is the variance of the correlation function in the *NVE* ensemble where energy does not fluctuate, a manifestly non-negative quantity. Therefore, the above equation recovers the lower bound Eq. (23), with a physically explicit expression for the missing piece. The relative contribution of the two terms determining  $\chi_4^{NVT}$  will be discussed in concrete cases in Secs. III and IV.

### 3. Local vs. global fluctuations

The above discussion may appear at first puzzling for the following reason: we have seen that the susceptibility  $\chi_4(t)$  is the space integral of a four-point correlation function  $G_4(\mathbf{y}, t)$  which, although developing some spatial correlations on approaching the glass transition, remains relatively short-range in the supercooled liquid phase and should not depend on far away boundary conditions that ultimately decide whether energy is conserved or not. If  $G_4(\mathbf{y}, t)$  does not depend, in the thermodynamic limit, on the ensemble, how can its integral over space,  $\chi_4(t)$ , be affected by the choice of ensemble? The answer is that while the finite volume corrections to  $G_4(\mathbf{y}, t)$  for a given  $\mathbf{y}$  tend to zero when  $V \rightarrow \infty$ , the integral over space of these corrections remain finite in that limit [54], and explain the difference between  $\chi_4^{NVT}$  and  $\chi_4^{NVE}$ . We understand that the physical correlation volume is given by  $\chi_4^{NVT}$ ; the long-range nature of the fixed energy constraint leads to an underestimate of  $\chi_4$  in the *NVE* ensemble, which is irrelevant to describe local correlations. This is particularly important in numerical simulations [54]: the study of the Fourier transform of  $G_4(\mathbf{y}, t)$ ,  $\hat{G}_4(\mathbf{q}, t)$  in the *NVE* ensemble will lead to a singular behavior associated to the fact that  $\lim_{q \rightarrow 0} \hat{G}_4(\mathbf{q}, t) \neq \hat{G}_4(\mathbf{q} = 0, t)$ , whereas the two coincide only in the most general ensemble where all conserved quantities are let free to fluctuate. The former quantity is independent of the ensemble and will be denoted  $\chi_4^*$  in the following, whereas the latter depends on the macroscopic constraint.

### 4. Various sources of fluctuations

Equation (35) makes precise the intuition that dynamic fluctuations are partly induced by the fluctuations of quantities that physically affect the dynamic behavior [1, 55]. Among these quantities, some are conserved thermodynamic quantities, such as the energy or density,

and the dependence of the dynamics on those quantities are simply measured by the derivatives of the correlation function. The contribution of the local fluctuations of these quantities can therefore be estimated and lead to a lower bound to the total dynamic fluctuations. In a supercooled liquid one expects on general grounds that energy and density should play major roles in the dynamics. From the thermodynamic theory of fluctuations [56], we know that in fact temperature (seen formally as a function of energy and density) and density are independent random variables, with variance  $\langle \delta T^2 \rangle = T^2/(Nc_V)$  and  $\langle \delta \rho^2 \rangle = k_B T \kappa_T / (N \rho_0)$ . Therefore Eq. (35) gives for the “true” dynamic susceptibility:

$$\chi_4^* = \frac{1}{c_V} \left( \frac{\partial C_o}{\partial \ln T} \right)^2 + \rho_0 k_B T \kappa_T \left( \frac{\partial C_o}{\partial \ln \rho} \right)^2 + \chi_4^{NVE}, \quad (44)$$

The question of whether other, “hidden” variables also contribute to the dynamic fluctuations is tantamount to comparing  $\chi_4^{NVE}$  with  $\chi_4^*$ . This question is very difficult to resolve theoretically in general. The rest of this paper and the companion paper [37] are devoted to theoretical arguments and numerical simulations which attempt to clarify this issue. The outcome is important for the physics of glassy media, since  $\chi_4^{NVE} < \chi_4^*$  would mean that most of the dynamics heterogeneities as measured by  $\chi_4$  are in fact induced by static energy and/or density inhomogeneities. Whether energy or density fluctuations is the dominant factor can be assessed by comparing the two explicit terms appearing in the right hand side of Eq. (44). Assuming time-temperature superposition, the ratio  $r$  of the two terms for  $t = \tau_\alpha$  reads:

$$r = \rho_0 c_V k_B T \kappa_T \left( \frac{\frac{d \ln \tau_\alpha}{d \ln \rho} |_T}{\frac{d \ln \tau_\alpha}{d \ln T} |_T} \right)^2. \quad (45)$$

Following Ref. [57], and noting that  $\rho_0 c_V k_B T \kappa_T \ll 1$  in usual liquids, we conclude that for most glass-formers,  $r$  is significantly less than one, which means that density effects are weaker than temperature effects and consequently contribute little to dynamic heterogeneities. The situation is of course completely the opposite in hard-sphere colloidal glasses, where  $d \ln \tau_\alpha / d \ln T |_T \rightarrow 0$  and  $r \gg 1$ .

## F. Summary

After motivating the use of multi-point correlation functions to detect non-trivial dynamic correlations in amorphous materials, we discussed the idea that induced fluctuations are more easily accessible experimentally than spontaneous ones, and can be related to one another by fluctuation-dissipation theorems. Elaborating on this idea, we have shown that the derivative of the correlation function with respect to temperature or density directly gives access to a correlation volume  $\chi_T$  or  $\chi_\rho$ , defined from the correlation between local energy or

density fluctuations and the dynamics. This relation can be used to show on very general grounds that a rapid slowing down of the dynamics must be accompanied by the growth of a correlation volume. The detailed relation between this correlation volume and a correlation length-scale however depends on the detailed spatial structure of the correlation function.

We have then showed that the dynamic four-point susceptibility depends in general on the chosen statistical ensemble. In the case where conserved variables are allowed to fluctuate, we showed that the dynamic four-point susceptibility is bounded from below by terms that capture the contribution of energy and density fluctuations to dynamic heterogeneities. Our central results, enabling one to estimate a dynamic correlation volume from experiments, are given in Eqs. (16, 23, 25, 44). Whereas we expect that for most supercooled liquids, the contribution of temperature is the dominant effect, the quality of our bounds as quantitative estimators of  $\chi_4$ , and their physical relevance is, at this stage of the discussion, an open question which we carefully address below and in the companion paper [37]. The following section is devoted to a quantitative study of this question within a field-theory formalism. A surprising outcome of this analysis is that four-point correlations not only depend on the chosen statistical ensemble, but also on the choice of microscopic dynamics (Newtonian or stochastic).

### III. ENSEMBLE AND DYNAMICS DEPENDENCE OF DYNAMICAL FLUCTUATIONS: A FIELD-THEORETICAL PERSPECTIVE

In the following we develop in detail an approach to dynamical fluctuations in supercooled liquids based on field-theory techniques, and discuss how the ensemble dependence of dynamic fluctuations, discussed in the previous sections, can be understood from a diagrammatic point of view. This is important since any self-consistent resummation/approximation scheme must be compatible with the bounds derived above. Furthermore, we unveil that, contrary to the behavior of correlators measuring the average dynamics, dynamic fluctuations depend on the dynamics in a remarkable way. Simplification can occur if a dynamical critical point exists, as in mode-coupling theory. In the companion paper [37] we will point out how these simplifications occur in such cases. In the following we aim to keep the discussion more general than the confines of mode-coupling theory or any other particular theoretical approach.

#### A. The dynamic field-theory

##### 1. A reminder of the usual static case

The dynamic field-theory strategy is analogous to the one used for ordinary (static) critical phenomena which we now recall, focusing on the ferromagnetic Ising transition as a simple example [58]. The starting point is the Legendre functional transform  $\Gamma(m(\mathbf{x}))$  of the free energy  $\beta F(h(\mathbf{x}))$ , itself defined as a functional of the magnetic field  $h(\mathbf{x})$ :

$$\Gamma(m(\mathbf{x})) = \beta F(h(\mathbf{x})) - \int d\mathbf{x}' h(\mathbf{x}') m(\mathbf{x}'), \quad (46)$$

where  $h(\mathbf{x})$  on the right hand side is the field that leads to the magnetization profile  $m(\mathbf{x})$ . The magnetization is determined via the equation:

$$m(\mathbf{x}) = \frac{\delta \beta F}{\delta h(\mathbf{x})}. \quad (47)$$

Two important properties of the functional  $\Gamma(m(\mathbf{x}))$  that can be directly derived using the previous relation are:

$$\begin{aligned} \frac{\delta \Gamma}{\delta m(\mathbf{x})} &= -h(\mathbf{x}), \\ \frac{\delta^2 \Gamma}{\delta m(\mathbf{x}) \delta m(\mathbf{x}')} &= \frac{\delta h(\mathbf{x})}{\delta m(\mathbf{x}')} \equiv [\langle s(\mathbf{x})s(\mathbf{x}') \rangle]^{-1}. \end{aligned} \quad (48)$$

The last exact identity indicates that the operator obtained by differentiating the functional  $\Gamma$  twice is the inverse of the spin-spin correlation function (considered as an operator). Note that these are simple generalizations of usual thermodynamic relations.

In general one cannot compute  $\Gamma$  exactly, but one can guess its form using symmetry arguments, and compute it approximately in a perturbative (diagrammatic) expansion in some parameter. Using the above identities, no further approximation is needed to obtain correlation functions. In its simplest version,  $\Gamma$  corresponds to the Ginzburg-Landau free energy functional. The saddle point equation for the magnetization then leads to the mean-field description of the transition, whereas the second derivative term gives the mean-field result for the spin-spin correlation function, valid when the space dimensionality is sufficiently large.

In the following, we will present a theory of dynamic fluctuations within a field-theoretic framework similar to the above static formalism. The main difference is that in the context of glassy dynamics, the relevant order parameter is no longer a one-point function like the magnetization but instead a two-point dynamic function which has to be introduced as an effective degree of freedom in the dynamic free-energy functional.

##### 2. Dynamic free-energy functionals and fluctuations

Different dynamic field-theories have been used in the literature to analyze the dynamics of dense liquids. The

common strategy is to write down exact or phenomenological stochastic equations for the evolution of the slow conserved degrees of freedom. For instance, for Brownian dynamics the only conserved quantity is the local density (energy and momentum are not conserved). The equation for the local density is in that case the so-called Dean-Kawasaki equation [59, 60], which can be derived exactly for Langevin particles (see Refs. [61, 62] for a discussion of different field-theories associated with such dynamics). In general, the field-theory associated to a given stochastic dynamics is obtained through the Martin-Siggia-Rose-deDominicis-Janssen method, where one first introduces response fields enforcing the correct time evolution and then averages over the stochastic noise [58, 61].

We will use a general notation that will allow us to treat all field theories proposed in the literature [61, 62] on the same footing. In all those field theories one has a set of slow conserved fields,  $\phi_i$  ( $i = 1, \dots, m$ ), and the corresponding response fields,  $\hat{\phi}_i$  arising from the Martin-Siggia-Rose procedure [63]. It will also be useful to put  $\phi_i, \hat{\phi}_i$  into a single  $2m$  dimensional vector  $\Phi_a$ ,  $a = 1, \dots, 2m$ . The average over the dynamic action of  $\Phi_a$  will be denoted  $\Psi_a$ :  $\langle \Phi_a \rangle = \Psi_a$ . As in the static case, the starting point of the analysis is a Legendre functional (also called the generator of two-particle irreducible diagrams or Baym-Kadanoff functional) [58, 64, 65]. It is equal to:

$$\Gamma(\Psi_a, G_{a,b}) = -\ln \int \mathcal{D}\Phi_a \exp \left( -S(\{\Phi_a\}) - \int dt d\mathbf{x} \sum_{a=1}^{2n} h_a(\mathbf{x}, t) [\Phi_a(\mathbf{x}, t) - \Psi_a(\mathbf{x}, t)] \right) \quad (49)$$

$$- \frac{1}{2} \int dt dt' d\mathbf{x} d\mathbf{x}' \sum_{a,b=1}^{2n} K_{a,b}(\mathbf{x}, t; \mathbf{x}', t') [\Phi_a(\mathbf{x}, t) \Phi_b(\mathbf{x}', t') - \Psi_a(\mathbf{x}, t) \Psi_b(\mathbf{x}', t') - G_{a,b}(\mathbf{x}, t; \mathbf{x}', t')] \right), \quad (50)$$

where  $S$  is the action of the field theory,  $h_a$ 's are such that  $\langle \Phi_a \rangle = \Psi_a$  and  $K_{a,b}$  imposes a certain value for the two-point functions:  $\langle \Phi_a \Phi_b \rangle - \Psi_a \Psi_b = G_{a,b}$ . The properties of  $\Gamma(\Psi_a, G_{a,b})$  are the same as in the static case because formally it is the same mathematical object. The only difference is that the dynamical functional depends on a larger number of variables. The difficulty is to devise an approximate expression for the functional  $\Gamma$ . Once this is done, one should differentiate the functional once to obtain self-consistent equations for the order parameters  $\Psi_a, G_{a,b}$  and twice to obtain (after inversion) and expression for their fluctuations. More precisely, we introduce the following matrix of second derivatives:

$$\partial^2 \Gamma = \begin{bmatrix} \frac{\delta \Gamma}{\delta G_{a,b} \delta G_{c,d}} & \frac{\delta \Gamma}{\delta G_{a,b} \delta \Psi_e} \\ \frac{\delta \Gamma}{\delta \Psi_f \delta G_{a,b}} & \frac{\delta \Gamma}{\delta \Psi_e \delta \Psi_f} \end{bmatrix} \equiv \begin{bmatrix} A & B \\ B^\dagger & C \end{bmatrix},$$

where we have introduced three block matrices  $A, B, C$ , in full correspondence with those introduced above in Sec. II E 1. The inversion of  $\partial^2 \Gamma$  in the “ $GG$ -sector” allows one to obtain the objects of interest in this paper, namely the four-point space-time correlation functions:

$$(\partial^2 \Gamma)_{a,b;c,d}^{-1,G} = \langle (\Phi_a(\mathbf{x}, t) \Phi_b(\mathbf{x}', t') - \Psi_a(\mathbf{x}, t) \Psi_b(\mathbf{x}', t')) \times (\Phi_c(\mathbf{y}, s) \Phi_d(\mathbf{y}', s') - \Psi_c(\mathbf{y}, s) \Psi_d(\mathbf{y}', s')) \rangle_c, \quad (51)$$

where  $\langle \cdot \rangle_c$  means that we are focusing on the connected component. Similar relations hold for the second derivatives in the other sectors ( $G\Psi$  and  $\Psi\Psi$ ).

At this stage, it is important to recall that the dynamical functional  $\Gamma$  has a direct diagrammatic expression

as [58, 64]:

$$\Gamma(\Psi, G) = -\frac{1}{2} \text{Tr} \log G + \frac{1}{2} \text{Tr} G_0^{-1} [G + \Psi\Psi] - \Phi_{2PI}(\Psi, G), \quad (52)$$

where  $\Phi_{2PI}(\Psi, G)$  is the sum of all two particle irreducible Feynman diagrams (that cannot be decomposed in two disjoint pieces by cutting two lines) constructed with the vertices of the theory and using the full propagator  $G$  as lines and  $\Psi$  as sources [58, 64, 65]. Both the internal indices and spatio-temporal arguments were skipped for simplicity. The first derivatives lead to the self-consistent equations for the order parameter. Since in dynamical field-theories for liquids the slow physical fields are in fact conserved quantities the equations  $\delta \Gamma / \delta \Psi_a = 0$  do not fix the values of the physical fields that have to be fixed by the initial conditions. On the other hand, they set to zero the average of the response fields and enforce translational invariance [81].

On the other hand, the derivatives  $\delta \Gamma / \delta G = 0$  lead to formally exact self-consistent equations for the two-point correlation functions. These equations can be written as a Schwinger-Dyson matrix equation:

$$G^{-1} = G_0^{-1} - \Sigma(G), \quad \Sigma(G) = \frac{\delta \Phi_{2PI}}{\delta G},$$

where  $\Sigma$  is the self-energy. A given approximation consists in retaining a given set of diagrams in  $\Phi_{2PI}$ , or alternatively in  $\Sigma(G)$ . For example, mode-coupling theories generically consist in only retaining the “bubble”

diagram for  $\Sigma(G)$ , see Refs. [38, 61, 66] for detailed discussions, and [37] in the present context.

### B. Four-point correlation functions and ensemble dependence

From the above general inversion formulas for block matrices, Eqs. (40, 41), one can recast the inversion of  $\partial^2\Gamma$  in a form transparent both from physical and diagrammatic standpoints. Let us first discuss the simple case where the  $\Psi_a$ 's are identically zero by symmetry, as happens for instance in the  $p$ -spin model for which a gauge symmetry implies that the average value of the spins is always zero. In this case, the block matrix  $B$  is also zero by symmetry. Equation (40) then simplifies:

$$(\partial^2\Gamma)^{-1,G}_{a,b;c,d} = \left[ \frac{\delta^2\Gamma}{\delta G_{a,b}\delta G_{c,d}} \right]^{-1} \equiv A^{-1}. \quad (53)$$

In general this symmetry does not hold, in particular for liquids for which the analysis is more involved. However, it turns out that the fundamental object to consider is still  $A^{-1}$ , as we now explain.

As mentioned above, the equation determining the two-point correlators is  $\delta\Gamma/\delta G = 0$ . Therefore the variation of the value of  $G$  due to a small variation of  $\Psi$ , all

other parameters being kept fixed, is given by:

$$\frac{\delta G}{\delta \Psi} \delta \Psi = - \left[ \frac{\delta^2\Gamma}{\delta G \delta G} \right]^{-1} \frac{\delta^2\Gamma}{\delta G \delta \Psi} \delta \Psi \equiv -A^{-1} B \delta \Psi. \quad (54)$$

Using Eq. (41) and the bottom right part of the matrix inversion relation, Eq. (40), the four-point correlation functions can be written in a physically transparent way:

$$(\partial^2\Gamma)^{-1,G}_{a,b;c,d} = \left[ \frac{\delta^2\Gamma}{\delta G_{a,b}\delta G_{c,d}} \right]^{-1} + \sum_{e,f} \left( \frac{\delta G_{ab}}{\delta \Psi_e} \langle \Psi_e \Psi_f \rangle_c \left( \frac{\delta G_{cd}}{\delta \Psi_f} \right)^\dagger \right). \quad (55)$$

This expression parallels Eq. (44) in Sec. II, and the last term corresponds to the dynamic fluctuations induced by the fluctuations of conserved quantities. This formula is however much more general because it applies not only to  $\chi_4(t)$  but also to  $G_4(q,t)$ . Indeed, in Fourier space, the terms contributing to  $G_4(q,t)$  read:

$$\langle \delta \rho_{-k_3}(t) \delta \rho_{k_3+q}(0) \delta \rho_{-k_4}(t) \delta \rho_{k_4-q}(0) \rangle. \quad (56)$$

Therefore the extra contribution from conserved quantities, namely the last term in Eq. (55), reads:

---


$$\sum_{e,f} \int d\omega \frac{\partial \langle \delta \rho_{-k_3}(t) \delta \rho_{k_3+q}(0) \rangle}{\partial \Psi_e(\omega, q)} \langle \Psi_e(\omega, q) \Psi_f(-\omega, -q) \rangle_c \frac{\partial \langle \delta \rho_{-k_4}(t) \delta \rho_{k_4-q}(0) \rangle}{\partial \Psi_f(-\omega, -q)}. \quad (57)$$


---

Now, one should notice that all terms corresponding to indices in the response field sector of  $\Psi$  (i.e.  $e, f > m$ ) identically vanish at  $q = 0$ . The reason is that the response fields always appear in the vertices of the field-theory in the form  $\nabla \Psi$ . As a consequence, terms like  $\delta^2\Gamma/\delta G \delta \Psi_e(\omega, q)$ , for  $e > m$ , are proportional to  $q$  at small  $q$ .

In the case  $q = 0$ , the value of conserved fields such as  $\Psi_e(\omega, q)$  for  $e \leq m$  are by definition constant over time and set by initial conditions:  $\langle \Psi_e(\omega, q) \Psi_f(-\omega, -q) \rangle_c = V \delta(\omega) \Sigma_{ef}$  where  $\Sigma_{ef}$  are the correlators of thermodynamic fluctuations of all conserved quantities  $\Psi$ , determined by the probability distribution of initial conditions. As a consequence the term in Eq. (57) at  $q = 0$  precisely reduces to the form discussed in the previous section on general grounds for  $\chi_4(t) \equiv G_4(q = 0, t)$ :

$$\sum_{e,f=1}^m \frac{\partial \langle \delta \rho_{-k_3}(t) \delta \rho_{k_3}(0) \rangle}{\partial \Psi_e} \Sigma_{ef} \frac{\partial \langle \delta \rho_{-k_4}(t) \delta \rho_{k_4}(0) \rangle}{\partial \Psi_f}. \quad (58)$$

For Brownian dynamics density is the only conserved quantity and thus only one term,  $m = 1$ , contributes

to the sum in Eq. (58). In the case of Newtonian dynamics there are in principle  $2 + d$  conserved quantities, density, momentum and energy. However, by symmetry, the contribution of the momentum fluctuations is zero, and only density and energy should be considered. In  $p$ -spin disordered systems, on the other hand, this extra term is simply absent, and  $m = 0$ .

The conclusion is once again that the choice of statistical ensemble matters for determining four-point correlators. For  $q \neq 0$ , the extra terms Eq. (57) are in general always non-zero and contribute to  $G_4(q, t)$ . On the other hand, if one focuses on the case where  $q = 0$  exactly, the initial distribution is crucial. As an example, in the case of Newtonian dynamics in the  $NVE$  ensemble, all the extra contributions vanish since in that ensemble all conserved quantities are strictly fixed and  $\Sigma_{ef}^{NVE} \equiv 0$ . Thus, we find again within this formalism that the equality  $\lim_{q \rightarrow 0} G_4(q, t) = G_4(0, t)$  is valid only in the most general ensemble where all conserved quantities fluctuates. In more restricted ensembles, such as  $NVE$ , it is violated.

Let us now explore the diagrammatic content of

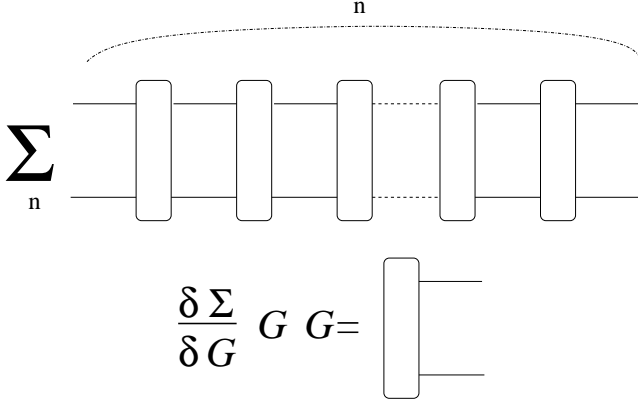


FIG. 2: Diagrammatic representation of the parquet diagrams obtained by expanding Eq. (59):  $(1 - \partial_G \Sigma G G)^{-1} = \sum_n (\partial_G \Sigma G G)^n$ .

Eq. (55). The first term can be rewritten using the general expression of  $\Gamma$  as:

$$\left[ \frac{\delta^2 \Gamma}{\delta G \delta G} \right]^{-1} = \left[ G^{-1} G^{-1} - \frac{\delta \Sigma(G)}{\delta G} \right]^{-1},$$

where the objects in the above expression are four-index matrices. This term can be rearranged as follows:

$$\begin{aligned} \left[ \frac{\delta^2 \Gamma}{\delta G \delta G} \right]_{a,b;c,d}^{-1} &\equiv \sum_{c',d'} G_{a,c'} G_{b,d'} \\ &\times \left( \delta_{c',c} \delta_{d',d} - \sum_{c'',d''} \frac{\delta \Sigma_{c'd'}(G)}{\delta G_{c'',d''}} G_{c'',c} G_{d'',d} \right)^{-1}. \end{aligned} \quad (59)$$

One can now formally expand the term in parenthesis as  $(1 - \partial_G \Sigma G G)^{-1} = \sum_n (\partial_G \Sigma G G)^n$  to recover the so-called ‘‘parquet’’ diagrams [65] that give a formally exact representation of the four-point function, see Fig. 2. We see that the role of these parquet diagrams is even more general. Actually, from Eq. (54) above, one sees that these diagrams are involved in the computation of the response of two-point correlators to a change in conserved quantities:

$$\chi_\Psi \equiv \frac{\delta G}{\delta \Psi} = - \left[ \frac{\delta^2 \Gamma}{\delta G \delta G} \right]^{-1} \frac{\delta^2 \Gamma}{\delta G \delta \Psi}. \quad (60)$$

This last expression shows that if all conserved quantities are fixed, such that the extra term Eq. (57) vanishes, the parquet diagrams will contribute both to  $\chi_4$  and to  $\chi_\Psi$ .

The second term in Eq. (55) also has a direct diagrammatic interpretation that is shown in Fig. 3. It consists of two parquets closed by three-leg vertices and joined by a correlation function of conserved variables. The wavevector  $q$  in  $G_4(q, t)$  is, in the diagrams, the wavevector flowing into the parquets and in the middle ‘‘link’’ corresponding to  $\langle \Psi_e \Psi_f \rangle_c$ , as it appears explicitly in Eq. (57). This general analysis is particularly useful in

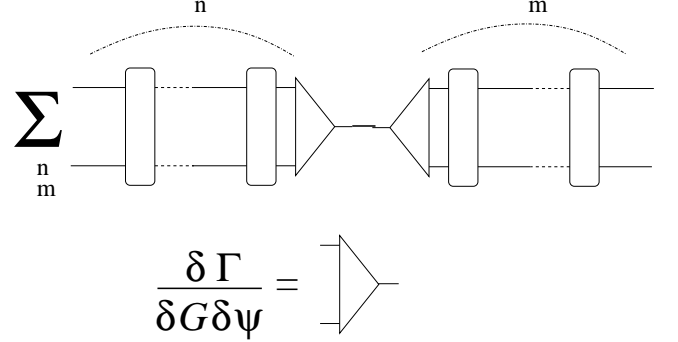


FIG. 3: ‘‘Squared-parquets’’ representation of the contribution of conserved quantity fluctuations to  $\chi_4$ . They correspond to the second term in Eq. (55).

the context of MCT but in cases where no divergence exists, we still expect that an analysis based on the general field-theoretic building blocks outlined in this section can be useful. For example, when a dynamical critical point is avoided or does not exist, the time-dependence of the (usually) non-singular three-leg vertex contribution  $\frac{\delta^2 \Gamma}{\delta G \delta \Psi}$  will also contribute to the temporal behavior of  $\chi_4$ .

### C. Consequence for physical observables and conclusions

As discussed in [16] MCT provide a simple approximation for parquet diagrams in which the self-energy is approximated by a bubble diagram. Within this approximation the parquet diagrams simplify into the ladder diagrams analyzed in [16], which diverge at the mode-coupling critical point.

In Ref. [16], however, only the ladder diagrams were analyzed. The contribution to  $G_4$  of Eq. (57) corresponding to the ‘‘squared ladders’’ was overlooked. As a consequence the MCT results in Ref. [16] for  $\chi_4(t) = G_4(q = 0, t)$  only apply close to the critical point in the following cases (see also [37] for further discussion):

- $NVE$  ensemble for Newtonian dynamics;
- $NVT$  ensemble for Brownian dynamics;
- $p$ -spin models.

On the other hand, whenever conserved quantities are allowed to fluctuate, or when considering  $G_4(q, t)$  at non-zero values of  $q$ , the contribution of (57) may be important. For example, within the context of MCT where  $\chi_\Psi$  diverges as  $\epsilon^{-1}$  (where  $\epsilon$  is the reduced distance from the critical point), the contribution of (58) in fact becomes dominant and  $\chi_4$  now diverges as  $\epsilon^{-2}$ .

As a consequence we expect that in general (not only within MCT)  $G_4(q, t)$  will receive contributions of different physical origin with possibly different temperature dependencies, and whose relative amplitude might even depend on the chosen microscopic dynamics (Brownian

or Newtonian). On the other hand, we see that the fundamental operator  $\partial^2\Gamma/\partial G\partial G$  governing the growth of dynamic correlations indeed corresponds to the ladder diagrams considered in Ref. [16]. Therefore it is both of theoretical and practical relevance to introduce a correlator with a physical content similar to that of  $G_4(q, t)$ , but unaffected by the presence of global conservation laws and therefore by the choice of statistical ensemble. An observable with those properties has been discussed recently [48]. It corresponds to the response of the intermediate scattering function  $G$  to a small inhomogeneous external potential  $V_{ext}$ . Within the previous formalism one finds:

$$\frac{\delta^2\Gamma}{\delta G\delta G} \frac{\delta G}{\delta V_{ext}} + \frac{\delta^2\Gamma}{\delta G\delta V_{ext}} + \frac{\delta^2\Gamma}{\delta G\delta\Psi} \frac{\delta\Psi}{\delta V_{ext}} = 0,$$

and therefore:

$$\frac{\delta G}{\delta V_{ext}} = - \left[ \frac{\delta^2\Gamma}{\delta G\delta G} \right]^{-1} \left( \frac{\delta^2\Gamma}{\delta G\delta V_{ext}} + \frac{\delta^2\Gamma}{\delta G\delta\Psi} \frac{\delta\Psi}{\delta V_{ext}} \right).$$

Since the source term on which the operator  $[\delta^2\Gamma/\delta G\delta G]^{-1}$  acts is expected to be weakly temperature and density dependent, one sees that this quantity gives an almost direct measure of the critical behavior of the dynamic correlations encoded in the operator  $[\delta^2\Gamma/\delta G\delta G]$ . When the external potential is homogeneous in space one finds a quantity proportional to  $\chi_\Psi$  [48], while for an inhomogeneous external potential one can probe the spatial structure of dynamic fluctuations. Indeed, when one differentiates with respect to the Fourier component  $V_{ext}(q)$ , the wavevector  $q$  plays the same role as for  $G_4$  [48]. This can alternatively be seen at the diagrammatic level because it is the wavevector entering into the ladders in Fig. 3.

The conclusion of this section is that four-point correlations not only depend on the *statistical ensemble* (for  $q = 0$ ) but, remarkably and perhaps unexpectedly, also on the *choice of dynamics*. This is to be contrasted with the case for two-point correlators, which are independent of the chosen ensemble and are known numerically to be independent of the dynamics, at least in the relevant “slow” regime [67, 68]. In a sense, this means that four-point correlations are not the best suited observables to characterize dynamic heterogeneity in glassy materials, since they mix several physical effects. A better observable is the response function  $\partial G/\partial V_{ext}$  discussed above.

Clear-cut statements with four-point quantities can however be made when the dynamic lengthscale grows dramatically at some finite temperature or density, as is the case within MCT where the operator  $\delta^2\Gamma/\delta G\delta G$  develops a zero mode that leads to a divergence of the dynamic lengthscale  $\xi$ . Close to the critical point, these statements may be summarized as follows [82]:

- $\chi_4(\tau_\alpha)$  for *NVT* Newtonian dynamics diverges more strongly than  $\chi_4(\tau_\alpha)$  for *NVT* stochastic dynamics;

- $\chi_4(\tau_\alpha)$  for *NVE* Newtonian dynamics diverges like  $\chi_4(\tau_\alpha)$  for *NVT* stochastic dynamics;
- $\chi_4(\tau_\alpha)$  for *NVE* Newtonian dynamics and *NVT* stochastic dynamics diverge like  $\chi_T(\tau_\alpha)$  (or  $\chi_\rho(\tau_\alpha)$ ).

However, these different divergences reflect the same underlying physics, which is the growth of a *unique* lengthscale  $\xi$  in all of these cases. Only the relation between  $\chi_4(\tau_\alpha)$  and  $\xi$  changes. This becomes clear when one considers the (ensemble-independent) function  $G_4(q, \tau_\alpha)$  for  $q \neq 0$ . In all of these cases,  $G_4(q, \tau_\alpha)$  can be written as a scaling function  $g_4(q\xi)$  with the same  $\xi$  but different functional forms. For example,  $g_4^N(q\xi)$  for Newtonian dynamics can be written as  $g_4^B(q\xi) + c_q[g_4^B(q\xi)]^2$ , where  $c_q$  is a coefficient and  $g_4^B(q\xi)$  the scaling function for Brownian dynamics, which can be obtained explicitly from the critical properties of  $(\delta^2\Gamma/\delta G\delta G)^{-1}$  [48]. Note that the relation between  $\chi_4(\tau_\alpha)$  for *NVE* Newtonian dynamics,  $\chi_4(\tau_\alpha)$  for *NVT* Brownian dynamics and  $\chi_T(\tau_\alpha)$  may not hold in non-critical cases, or in cases where no underlying critical point is present, as is likely the case in silica.

In the following section we will check all these statements (ensemble and dynamics dependence, unique lengthscale) using numerical simulations of two molecular glass-formers of different fragilities.

#### IV. NUMERICAL RESULTS FOR TWO MOLECULAR GLASS-FORMERS

We now present our numerical calculations of the dynamic susceptibility  $\chi_T(t)$ , its relation to  $\chi_4(t)$ , and the behavior of spatial correlations in two well-studied models of molecular glass-formers: a binary Lennard-Jones (LJ) mixture [69], considered as a simple model system for fragile supercooled liquids [8], and the Beest, Kramer, and van Santen (BKS) model, which is a simple description of the strong glass-former silica [70, 71]. A first motivation for these simulations is that all terms contributing to the dynamic fluctuations can be separately evaluated and quantitatively compared. Therefore, the claim made in Ref. [36] that  $\chi_T(t)$  yields direct experimental access to the four-point susceptibility can be quantitatively established. A second interesting feature is that the influence of the microscopic dynamics and statistical ensemble can be quantified in the simulations by keeping the pair potential unchanged but by switching from the energy conserving Newtonian dynamics to some stochastic dynamics which locally supplies energy to the particles. Finally spatial correlators and dynamic lengthscales can be directly evaluated in the simulations therefore confirming the link between dynamic susceptibilities and dynamical lengthscales.

### A. Models and technical details

The binary LJ system simulated in this work is a 80:20 mixture of  $N_A = 800$  and  $N_B = 200$  Lennard-Jones particles of types  $A$  and  $B$ , with interactions

$$\phi_{\alpha\beta}^{\text{LJ}}(r) = 4\epsilon_{\alpha\beta} \left[ \left( \frac{\sigma_{\alpha\beta}}{r} \right)^{12} - \left( \frac{\sigma_{\alpha\beta}}{r} \right)^6 \right], \quad (61)$$

where  $\alpha, \beta \in [A, B]$  and  $r$  is the distance between the particles of type  $\alpha$  and  $\beta$ . Interaction parameters  $\epsilon_{\alpha\beta}$  and  $\sigma_{\alpha\beta}$  are chosen to prevent crystallization and can be found in Ref. [69]. The length, energy and time units are the standard Lennard-Jones units  $\sigma_{AA}$  (particle diameter),  $\epsilon_{AA}$  (interaction energy), and  $\tau_0 = \sqrt{m_A \sigma_{AA}^2 / (48\epsilon_{AA})}$ , where  $m_A = m_B$  is the particle mass and the subscript  $A$  refers to the majority species. Equilibrium properties of the system have been fully characterized [69]. At the reduced density  $\rho_0 = 1.2$ , where all our simulations are carried out, the MCT transition has been conjectured to be in the vicinity of  $T_g \sim 0.435$  [69]. The slowing down of the dynamics,  $T \gtrsim 0.47$ , can be correctly described by mode-coupling theory, but this description eventually breaks down when lowering the temperature further,  $T \lesssim 0.47$  [69].

To check the generality of our results, we have also investigated the behavior of a second glass-former, characterized by a very different fragility. To this end, we simulate a material with an Arrhenius dependence of its relaxation time, namely silica. Various simulations have shown that a reliable pair potential to simulate silica is the one proposed by BKS [70, 71]. The functional form of the BKS potential is

$$\phi_{\alpha\beta}^{\text{BKS}}(r) = \frac{q_\alpha q_\beta e^2}{r} + A_{\alpha\beta} \exp(-B_{\alpha\beta} r) - \frac{C_{\alpha\beta}}{r^6}, \quad (62)$$

where  $\alpha, \beta \in [\text{Si}, \text{O}]$  and  $r$  is the distance between the ions of type  $\alpha$  and  $\beta$ . The values of the constants  $q_\alpha, q_\beta, A_{\alpha\beta}, B_{\alpha\beta}$ , and  $C_{\alpha\beta}$  can be found in Ref. [70]. For the sake of computational efficiency the short range part of the potential was truncated and shifted at 5.5 Å. This truncation also has the benefit of improving the agreement between simulation and experiment with regard to the density of the amorphous glass at low temperatures. The system investigated has  $N_{\text{Si}} = 336$  and  $N_{\text{O}} = 672$  ions in a cubic box with fixed size  $L = 24.23$  Å. The Coulombic part of the potential has been evaluated by means of the Ewald sum using a constant  $\alpha L = 10.177$ .

For both LJ and BKS models we have numerically integrated Newton's equations of motion using a velocity Verlet algorithm [51] using a timestep  $h^{\text{LJ}} = 0.01\tau_0$  and  $h^{\text{BKS}} = 1.6$  fs, respectively. Doing so we can measure spontaneous dynamic fluctuations in the microcanonical  $NVE$  ensemble. Before these microcanonical production runs, all systems are equilibrated using a stochastic heat bath for a duration significantly longer than the typical relaxation time,  $\tau_\alpha$ , implying that particles move over several times their own diameter during equilibration.

Production runs were at least larger than  $30\tau_\alpha$ , and statistical convergence for dynamic fluctuations was further improved by simulating 10 independent samples of each system at each temperature. Doing this for many temperatures in two molecular systems obviously represents a substantial numerical effort.

To check the influence of the microscopic dynamics, and in particular the role of the energy conservation, we have also performed stochastic simulations of the LJ system using two different techniques. Following Ref. [67], we have simulated Brownian dynamics where Newton's equations are supplemented by a random force and a viscous friction whose amplitudes are related by the fluctuation-dissipation theorem. The numerical algorithm used to integrate these Brownian equations of motion is described in Refs. [51, 67] using the time step of  $h_{\text{BD}}^{\text{LJ}} = 0.016\tau_0$  and the friction coefficient was set to  $\zeta = 10m\tau_0$ . We use the equilibrium configurations obtained by MD simulations as starting point for our production runs in Brownian simulations. Finally we have implemented a second stochastic dynamics, a standard Monte Carlo dynamics, with the LJ potential [72]. At time  $t$ , the particle  $i$ , located at the position  $\mathbf{r}_i(t)$ , is chosen at random. The energy cost  $\Delta E$  to move it to the new position  $\mathbf{r}_i(t) + \boldsymbol{\delta}$  is evaluated,  $\boldsymbol{\delta}$  being a random vector comprised in a sphere of radius  $\delta_{\text{max}} = 0.075$ . The Metropolis acceptance rate,  $p = \min(1, e^{-\beta\Delta E})$ , is then used to decide whether the move is accepted [51]. One Monte Carlo timestep represents  $N = N_A + N_B$  attempts to make such a move.

### B. Physical observables

Following previous work [15, 32, 33], we monitor the dynamical behavior of the molecular liquids through the self-intermediate scattering function,

$$F_s(\mathbf{k}, t) = \left\langle \frac{1}{N_\alpha} \sum_{j=1}^{N_\alpha} e^{i\mathbf{k} \cdot [\mathbf{r}_j(t) - \mathbf{r}_j(0)]} \right\rangle, \quad (63)$$

where the sum in Eq. (63) runs over one of the species of the considered liquid ( $A$  or  $B$  in the LJ, Si or O for silica). We denote by  $f_s(\mathbf{k}, t)$  the real part of the instantaneous value of this quantity, so that we have  $F_s(\mathbf{k}, t) = \langle f_s(\mathbf{k}, t) \rangle$ .

The four-point susceptibility,  $\chi_4(t)$ , quantifies the strength of the spontaneous fluctuations around the average dynamics by the variance,

$$\chi_4(t) = N_\alpha [\langle f_s^2(\mathbf{k}, t) \rangle - F_s^2(\mathbf{k}, t)]. \quad (64)$$

In principle,  $\chi_4(t)$  in Eq. (64) retains a dependence on the scattering vector  $\mathbf{k}$ . Since the system is isotropic, we circularly average (63) and (64) over wavevectors of fixed modulus. Note that the value of dynamical correlations depend on  $|\mathbf{k}|$  as shown in [31, 35]. A detailed analysis of this dependence has been performed in [49]

and will be further discussed in [37]. In the following we will focus only on the value of  $|\mathbf{k}|$  for which the dynamical correlations are more pronounced and that measure the correlation of the local dynamics. For the LJ system we will mainly consider results for  $|\mathbf{k}| = 7.21$  and for the BKS one  $|\mathbf{k}| = 1.7 \text{ \AA}^{-1}$ . These values respectively represent the typical distance between  $A$  particles, and the size of the  $\text{SiO}_4$  tetrahedra. As discussed above, we expect  $\chi_T(t)$  to depend on the chosen statistical ensemble,  $NVE$  or  $NVT$ , for Newtonian dynamics, and to depend also on which microscopic dynamics is chosen, stochastic or energy conserving.

To evaluate the temperature derivatives involved in

$$\chi_T(t) = \frac{\partial}{\partial T} F_s(\mathbf{k}, t), \quad (65)$$

we perform simulations at nearby temperatures,  $T$  and  $T + \delta T$ , and estimate  $\chi_T(t)$  through finite differencing,  $\chi_T(t) \approx \delta F_s(k, t)/\delta T$ , as illustrated by arrows in Fig. 1 in Sec. II. For this procedure to be effective, temperature differences must be small enough that linear response holds. Taking  $\delta T$  too small leads however to poor statistics. The smallest  $\delta T$  which might be used can be estimated by comparing the statistical noise of  $F_s(k, t)$  to the expected response  $\chi_T \times \delta T$ . This leads in our case to the typical lower bound  $\delta T/T > 0.005$ . We have typically used  $\delta T/T \approx 0.01$ , which is not far from the lower bound. For some selected temperatures, we have explicitly checked that linear response is satisfied by comparing results for  $2\delta T$ ,  $\delta T$  and  $\delta T/2$ .

It might be worth recalling that the value of  $\chi_T(t)$  does not depend on which ensemble ( $NVE$  or  $NVT$ ) is chosen for its computation, since ensemble equivalence obviously holds for this local observable. Much less trivial is our numerical finding that  $\chi_T(t)$  is also found to be the same for Newtonian, Brownian and Monte Carlo dynamics for times pertaining to the structural relaxation. This is because we detect no dependence of the (average) structural relaxation dynamics of the binary LJ system upon its microscopic dynamics, apart from an overall time rescaling. On the other hand, the short-time dynamics is different in the three cases. Our findings then confirm for Brownian dynamics, and extend for Monte Carlo dynamics, the results of Refs. [67, 68] about the independence of the *average* glassy dynamics upon the microscopic dynamics. We will see below that clear differences emerge at the level of the *dynamic fluctuations*.

### C. Amplitude of the dynamic fluctuations

In this paper, we restrict our analysis of the dynamic susceptibilities to the amplitude of the peaks observed in Fig. 1, meaning that we study dynamic fluctuations on a timescale  $t \approx \tau_\alpha$ . The time dependence of the fluctuations are studied in the companion paper, Ref. [37].

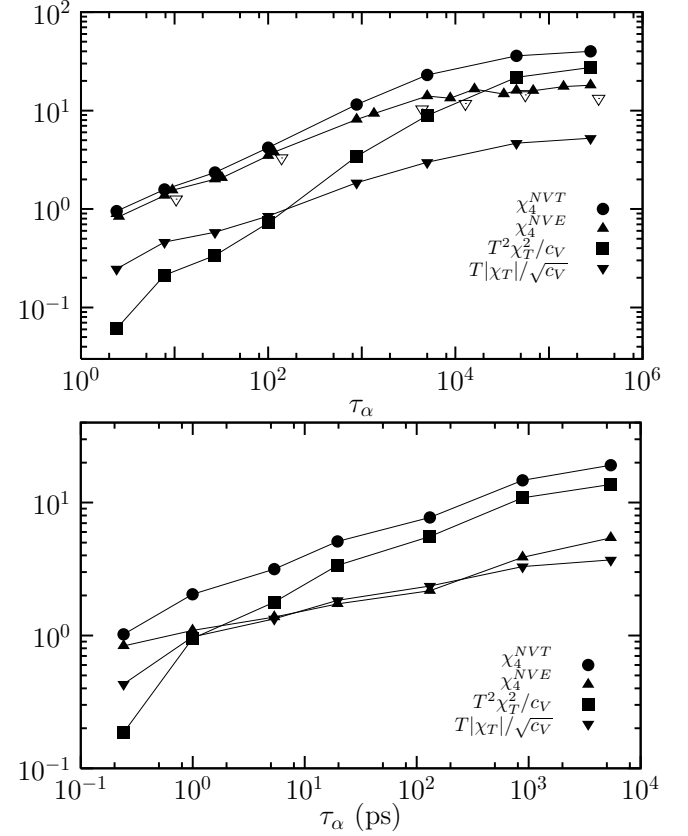


FIG. 4: Peak amplitude of various dynamic susceptibilities in the binary LJ mixture obtained from the  $A$  particles dynamics (top) and the BKS model for silica from the Si ions dynamics (bottom). Open triangles in the LJ system represent  $\chi_4^NVE$  measured in a smaller system with  $N = 256$  instead of the  $N = 1000$  used everywhere else in the paper. In both cases,  $T^2 \chi_T^2 / cv$  is smaller than  $\chi_4^NVE$  at high temperature, but increases faster and becomes eventually the dominant contribution to  $\chi_4^{NVT}$  in the relevant low temperature glassy regime. Note that the crossing occurs much earlier for BKS.

#### 1. Role of energy fluctuations in building dynamical correlations

Our results are summarized in Fig. 4, where we present our numerical data for  $T|\chi_T|/\sqrt{1/c_V}$ ,  $\chi_4^{NVE}$ ,  $T^2 \chi_T^2 / cv$  and the sum  $\chi_4^{NVT} = \chi_4^{NVE} + T^2 \chi_T^2 / cv$ , all quantities obtained from Newtonian dynamics simulations of both the LJ and BKS models. (Recall that we define  $c_V$  in units of  $k_B$  throughout this paper). When temperature decreases, all peaks shift to larger times and track the  $\alpha$ -relaxation. Simultaneously, their height increases, revealing increasingly stronger dynamic correlations as the glass transition is approached.

The main observation from the data displayed in Fig. 4, already announced in Ref [36], is that in both LJ and BKS systems the term  $T^2 \chi_T^2 / cv$  while being small,  $\sim O(10^{-1})$ , above the onset temperature of slow dynamics, grows much faster than  $\chi_4^{NVE}$  when the glassy regime is entered. As a consequence, there exists a temperature

below which the temperature derivative contribution to the four-point susceptibility  $\chi_4^{NVT}$  dominates over that of  $\chi_4^{NVE}$ , or is at least comparable. This crossover is located at  $T \approx 0.45$  in the LJ system,  $T \approx 4500$  K for BKS silica. Remarkably, the conclusion that  $T^2\chi_T^2/c_V$  becomes larger than  $\chi_4^{NVE}$  at low temperatures holds for both strong and fragile glass-formers, but for different reasons. In the LJ systems  $\chi_T$  increases very fast because timescales grows in a super-Arrhenius manner, which makes the temperature derivative larger and larger, while  $\chi_4^{NVE}$  saturates at low  $T$ . In the BKS system, although the temperature derivative is not very large because of the simple Arrhenius growth of relaxation timescales,  $\chi_4^{NVE}$  is even smaller [73], i.e. much smaller than in the fragile LJ system. It is interesting to note that the value of  $\chi_4^{NVE}$  and  $T^2\chi_T^2/c_V$  when they cross is substantially larger for the LJ system ( $\sim 10$ ) than for BKS ( $\sim 1$ ). Physically, this might be due to the fact that the  $T^2\chi_T^2/c_V$  contribution to dynamic correlations comes entirely from the energy conservation constraint. Therefore, this term is present even when relaxation occurs via a “local” Arrhenius process, as discussed in Section II.C. The  $\chi_4^{NVE}$  contribution, on the other hand, might capture more genuine “cooperative” effects, and hence be larger in more fragile systems.

It is important to remark that finite size effects could play a role in the present study: when measured in a system which is too small, dynamic fluctuations are underestimated [74]. Therefore it could be that using too small a system we have underestimated  $\chi_4^{NVE}$ , and therefore observed a fictitious saturation of the inequality (23). To investigate this possibility, we have included in Fig. 4 data for  $\chi_4^{NVE}$  obtained in a system comprising about 4 times less particles,  $N = 256$ , with essentially similar results. We have checked that also the average dynamics is unchanged when  $N = 256$ , so that  $\chi_T$  is not affected by finite size effects either. We are therefore confident that the main conclusion drawn from Fig. 4 is not an artifact due to finite size effects.

Two important conclusions follow from this observation. Firstly, we can safely conclude that  $T^2\chi_T^2/c_V$  is a very good approximation to  $\chi_4^{NVT}$  for relaxation times larger than  $\tau_\alpha \approx 10^4$  in the LJ system,  $\tau_\alpha \approx 10$  ps in BKS silica. Our results indicate that this becomes an even better approximation as temperature is lowered. As reported in Ref. [36], this opens suggests a direct experimental determination of  $\chi_4$  close to the glass transition temperature,  $T_g$ . Our data indicate however, that care must be taken when analyzing the first few decades of the dynamical slowing down where all terms contribute differently to  $\chi_4^{NVT}$ , and have different temperature dependences [36, 49, 75].

A second conclusion drawn from Fig. 4 concerns the physical origin of the dynamic heterogeneity in glass-forming liquids. Our observation that the term involving  $\chi_T^2$  gives the major contribution to  $\chi_4$ , directly implies, using the fluctuation-dissipation relation Eq. (16), that the local fluctuations of the energy are the main source

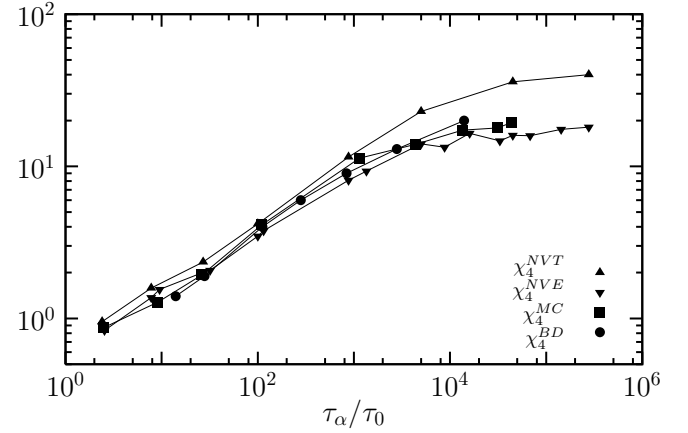


FIG. 5: Amplitude of four-point susceptibilities  $\chi_4(\tau_\alpha)$  obtained from the  $A$  particles dynamics in the LJ system for Newtonian canonical ( $\chi_4^{NVT}$ ), microcanonical ( $\chi_4^{NVE}$ ) dynamics and stochastic Monte Carlo ( $\chi_4^{MC}$ ) and Brownian ( $\chi_4^{BD}$ ) dynamics. Stochastic dynamics measurements follow the results obtained from microcanonical Newtonian dynamics, while the amplitudes obtained in the canonical ensemble for Newtonian dynamics are much larger, as predicted in Sec. III.

for the spatial fluctuations of the local dynamical behavior. However, as we argued above, this could well mean that the crossing between  $T^2\chi_T^2/c_V$  and  $\chi_4$  in fact occurs closer to  $T_g$  for more fragile systems. This would then lead to a systematic underestimation of  $\chi_4$  as a function of fragility.

## 2. Dynamics dependence of dynamical correlation

We conclude this section with a discussion of the data for dynamic fluctuations obtained through our stochastic simulations. The temperature evolution of the dynamic susceptibilities  $\chi_4(\tau_\alpha)$  obtained with Monte Carlo and Brownian dynamics are shown in Fig. 5 where it is compared to the data obtained in both canonical and microcanonical ensembles with Newtonian dynamics. Our data unambiguously show that dynamic fluctuations with stochastic dynamics are different from the ones obtained with Newtonian dynamics in the *NVT* ensemble. They are however very similar to the microcanonical ones. This result is not immediately intuitive because one could have imagined that stochastic simulations are a good approximation to the dynamics of liquids in the canonical ensemble. However, we have shown in Sec. III that this naive expectation is in fact incorrect. The absence of the energy conservation in the stochastic dynamics (MD or BD) removes the contribution of the “squared parquets” and leads to  $\chi_4^{NVE} \sim \chi_4^{BD} \sim \chi_4^{MC}$ . This is in excellent agreement with our numerical data.

Another confirmation of our theoretical expectations is presented in Fig. 6 in which we show the time dependence of  $\chi_4$  for *NVE* Newtonian dynamics, *NVT* Brownian,

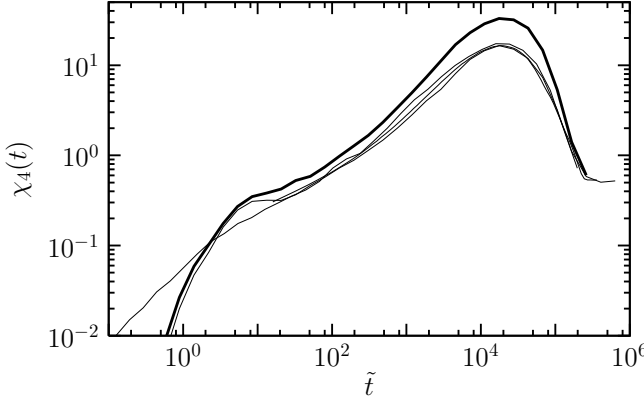


FIG. 6: Four-point susceptibilities at  $\chi_4(t)$  at  $T = 0.45$  obtained from the  $A$  particles dynamics in the LJ system for Newtonian canonical (shown as a thicker line), microcanonical dynamics and stochastic Monte Carlo and Brownian dynamics as a function of a rescaled time chosen so that all  $\chi_4$ 's overlap near the alpha relation. We chose  $\tilde{t} = t$  for  $NVE$  Newtonian dynamics,  $\tilde{t} = t/24$  for Brownian dynamics,  $\tilde{t} = t/100$  for Monte Carlo dynamics. The Newtonian  $\chi_4^{NVT}(t)$  is larger than the others, which are all nearly identical in both beta and alpha regimes.

Monte-Carlo and Newtonian dynamics. The first three curves are essentially identical in the late-beta and alpha-regimes whereas the last one is clearly larger. Although this dependence on the microscopic dynamics is a clear-cut prediction in the context of MCT, as discussed also in [37], our previous general diagrammatic discussion shows that this should hold more generally.

Another interesting consequence of our diagrammatic analysis is that  $\chi_T$  and  $\chi_4^{NVE}$  should have a similar critical scaling in temperature and time. Again this holds exactly within MCT but it is expected also in general if the three-leg vertex does not introduce any additional singular behavior. In fact, as discussed in the previous sections,  $\chi_T$  consists of a parquet diagram closed by a three-leg vertex whereas  $\chi_4^{NVE}$  is given by single parquet diagrams. In Fig. 4 we confirm numerically that the peaks of  $\chi_T$  and  $\chi_4^{NVE}$  scale in the same way with the temperature. This similarity should in fact extend to the whole time dependence but the results are less satisfactory, as discussed in the companion paper [37]. This might be due to pre-asymptotic effects at short times.

#### D. Spatial correlations

We now discuss the spatial correlations associated with the global fluctuations measured through  $\chi_T(t)$  and  $\chi_4(t)$ . To this end, we define the local fluctuations of the dynamics through the spatial fluctuations of the instantaneous value of the self intermediate scattering function,

$$\delta f_k(\mathbf{x}, t) = \sum_i \delta(\mathbf{x} - \mathbf{r}_i(0)) \cos[\mathbf{k} \cdot (\mathbf{r}_i(t) - \mathbf{r}_i(0))] - \rho_0 F_s(\mathbf{k}, t). \quad (66)$$

In the following, we will drop the  $\mathbf{k}$  dependence of the dynamic structure factors to simplify notations. Local fluctuations of the energy at time  $t$  are defined as usual,

$$\delta e(\mathbf{x}, t) = \sum_i \delta(\mathbf{x} - \mathbf{r}_i(t)) e_i(t) - \rho_0 e, \quad (67)$$

where  $e_i(t) = mv_i^2(t)/2 + \sum_j V(r_{ij}(t))$  is the instantaneous value of the energy of particle  $i$ , and  $e \equiv \langle N^{-1} \sum_i e_i \rangle$  is the average energy per particle.

Spontaneous fluctuations of the dynamics can be detected through the “four-point” dynamic structure factor,

$$S_4(\mathbf{q}, t) = \frac{1}{N} \langle \delta f(\mathbf{q}, t) \delta f(-\mathbf{q}, t) \rangle, \quad (68)$$

while correlation between dynamics and energy are quantified by the following “three-point” function,

$$S_T(\mathbf{q}, t) = \frac{1}{N} \langle \delta f(\mathbf{q}, t) \delta e(-\mathbf{q}, t = 0) \rangle. \quad (69)$$

In Eqs. (68, 69),  $\delta f(\mathbf{q}, t)$  and  $\delta e(\mathbf{q}, t)$  denote the Fourier transforms with respect to  $\mathbf{x}$  of  $\delta f(\mathbf{x}, t)$  and  $\delta e(\mathbf{x}, t)$ , respectively. We will show data for fixed  $|\mathbf{k}|$ , as for the dynamic susceptibilities above. In our numerical simulations we have also performed a circular averaging over wavevectors of fixed moduli  $|\mathbf{q}|$ , although the relative orientations of  $\mathbf{q}$  and  $\mathbf{k}$  plays a role [17, 76].

We present our numerical results for the temperature dependence of four-point and three-point structure factors in Fig. 7. Similar four-point dynamic structure factor have been discussed before [7, 14, 15, 19, 30, 31, 32, 33]. They present at low  $q$  a peak whose height increases while the peak position shifts to lower  $q$  when  $T$  decreases. This peak is unrelated to static density fluctuations which are small and featureless in this regime [69]. This growing peak is direct evidence of a growing dynamic lengthscale,  $\xi_4(T)$ , associated to dynamic heterogeneity as temperature is decreased. The dynamic lengthscale  $\xi_4$  should then be extracted from these data by fitting the  $q$ -dependence of  $S_4(q, t)$  to a specific form. An Ornstein-Zernike form has often been used [31, 32], and we have presented its  $1/q^2$  large  $q$  behavior in Fig. 7. Since our primary aim is to measure dynamic susceptibilities on a wide range of temperatures, we have used a relatively small number of particles,  $N = 1000$ . At density  $\rho_0 = 1.2$ , the largest distance we can access in spatial correlators is  $L/2 \approx 5$ , which makes an absolute determination of  $\xi_4$  somewhat ambiguous. Similarly the range of wavevectors shown in Fig. 7 is too small to assign a precise value even to the exponent characterizing the large  $q$  behavior of  $S_4(q, t) \sim 1/q^\alpha$ . Our data is compatible with a value  $\alpha \approx 2.4$ . To extract  $\xi_4$  we therefore

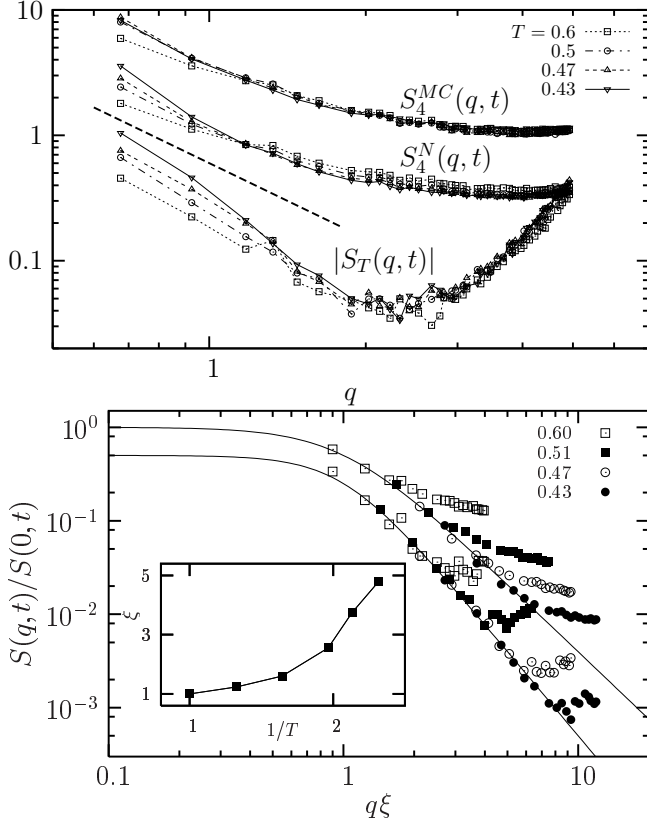


FIG. 7: Top: Four-point dynamic structure factors from Eqs. (68) for Monte Carlo (MC) and Newtonian (N) dynamics, and three-point structure factor, Eq. (69), for Newtonian dynamics. For comparison, we show the power law  $1/q^2$  as a dashed line. Note that  $S_T$  is a negative quantity, so we present its absolute value.  $S_T$  and  $S_4^{MC}$  have been vertically shifted for graphical convenience. Bottom: Rescaled dynamic structure factor for Newtonian dynamics using Eq. (70) with  $\alpha = 2.4$  for  $S_4$  and  $\alpha = 3$  for  $S_T$ . The same dynamic lengthscale  $\xi_4 = \xi_T \equiv \xi$  is used in both cases, and the evolution of  $\xi(T)$  is shown in the inset.

fix  $\alpha = 2.4$  and determine  $\xi_4$  by assuming the following scaling behavior [33],

$$S_4(q, t) = \frac{S_4(q = 0, t)}{1 + (q\xi_4)^\alpha}, \quad (70)$$

using  $S_4(0, t)$  and  $\xi_4$  as free parameters. The results of such an analysis are shown in the bottom panel of Fig. 7. This procedure leads to values for  $\xi_4$  which are in good agreement with previous determinations using different procedures [32]. In particular we find that a power law relationship  $\xi_4 \sim \tau_\alpha^{1/z}$  with  $z \approx 4.5$  describes our data well, as reported in Ref. [15] for this system.

Since dynamic structure factors probe local spatial correlations they do not depend on the statistical ensemble chosen for their calculation, at least in the thermodynamic limit. However, as predicted in Sec. III, dynamic correlations are expected to retain a dependence on the microscopic dynamics of the particles, our prediction be-

ing that correlations should be stronger for Newtonian dynamics than for stochastic dynamics. This prediction is directly confirmed in Fig. 7 where we show  $S_4^{MC}(q, t)$  obtained from our Monte Carlo simulations. Clearly the temperature evolution of  $S_4^{MC}$  is much slower than that of  $S_4^{ND}$ , in agreement with the slower temperature evolution of  $\chi_4^{MC}$  already observed in Fig. 5.

An important new result contained in Fig. 7 is the presence and development of a similar low- $q$  peak in the three-point structure factor  $S_T(q, t)$ . Note that, as for  $\chi_T(t)$ , we find that  $S_T(q, t)$  is a negative quantity. This means that a local positive fluctuation of the energy is correlated to a local negative fluctuation of the two-time dynamics, i.e. to a locally faster than average dynamics. Therefore the (negative) peak in  $S_T(q, t)$  is a direct microscopic demonstration that dynamic heterogeneity is strongly correlated to the fluctuations of at least one local structural quantity, namely the energy [36]. When temperature decreases, the height of the peak in  $|S_T(q, t)|$  increases and its position shrinks towards lower  $q$ . This is again the sign of the presence of a second growing dynamic lengthscale,  $\xi_T$ , which reflects the extent of the spatial correlations between energy and dynamical fluctuations. Again an absolute determination of  $\xi_T$  is very hard due to system size limitations. Since we expect  $\xi_T$  and  $\xi_4$  to carry equivalent physical content, we have checked that our data are compatible with both lengthscales being equal. In Fig. 7, we rescale the three-point dynamic structure factor using Eq. (70) with  $\alpha = 3$ , and constraining  $\xi_T = \xi_4$ . The scaling is of similar quality, see the bottom panel in Fig. 7.

The local correlation between energy fluctuations dynamic heterogeneity is broadly consistent with several theoretical predictions (see also the companion paper [37] for further discussion). As mentioned in Sec. III the equality between  $\xi_T$  and  $\xi_4$  is a natural prediction of MCT calculations. This is also very natural from the point of view of kinetically constrained models [40]. Spin facilitated models, in particular, *postulate* such a correlation through the concept of dynamic facilitation: mobile sites carry positive energy fluctuations and through activated diffusion trigger the relaxation of neighboring sites [77]. In this picture a localized energy fluctuation affects the dynamics of a large nearby region so that there is not a one-to-one correspondence between slow and low-energy sites. There is therefore no contradiction between our results and the lack of correlation between “dynamic propensity” and local potential energy recently reported in Ref. [78].

## E. Summary

In this section we have discussed in detail the results of molecular dynamics simulations of a strong and a fragile glass-forming liquid. Our main contribution is the simultaneous measurement of spontaneous and induced dynamic fluctuations, and the quantitative confirmation

in two realistic liquids of the central claim announced in Ref. [36]: it is possible to obtain a quantitative estimate of the amplitude of dynamic fluctuations in supercooled liquids through the measurement of the quantity  $T^2\chi_T^2/c_V$ , which represents the major contribution to the fluctuations in the low temperature regime, see Fig. 4. We have directly measured in the Lennard-Jones system three- and four-point dynamic structure factors that display slightly different wavevector dependences but lead nevertheless to consistent quantitative estimates of a dynamic correlation lengthscale. This last result is very important since this is direct confirmation that an experimental estimate of a dynamic lengthscale, as performed in Ref. [36], is meaningful. Finally, we have found that, as predicted theoretically, four-point dynamic correlations are strongly dependent on the microscopic dynamics, at variance with usual two-point correlations.

## V. PERSPECTIVES AND CONCLUSIONS

We conclude this rather long article (to be followed by a companion paper) with brief comments. The main message that we aim to convey is that dynamical correlations depend on statistical ensembles, which has allowed us to establish relations and bounds between spontaneous fluctuations and induced ones, the latter being directly accessible to experiments [36]. Furthermore, through numerical simulations and theoretical arguments we have shown that dynamical correlations are mainly driven by structural (energy) fluctuations both in strong and fragile supercooled liquids. Finally, we have discovered that contrary to the average dynamics, dynamical correlations depend on the choice of microscopic dynamics. But they do so only through conserved quantities: Brownian and

Monte-Carlo dynamics lead to very similar quantitative results, whereas Newtonian dynamics leads to strong amplification of dynamical fluctuations. Physically, this can be ascribed to the fact that in the latter case, energy has to flow from one region of the system to another, leading to strong dynamic heterogeneities that cannot “heal” easily.

A companion paper [37] will be devoted to discussing the same issues within different theoretical frameworks: mean-field spin glass models [38], mode-coupling theory [39], kinetically constrained models [40], as well as a comparison of these theoretical predictions with numerical simulations.

As for the perspective for the future, we hope that our work will trigger more experimental and numerical investigations of supercooled liquids and jamming systems, extending our results both from a quantitative and a qualitative point of view. In particular, the distinction between dynamical correlations and cooperativity, if any, should be clarified. This could be relevant to justify the identification of  $\chi_4$  with its lower bound for fragile systems. The analysis of similar issues in out-of-equilibrium situations (such as aging or sheared systems) is certainly worth pursuing.

## Acknowledgments

We thank L. Cipelletti, S. Franz, F. Ladieu, D. L’Hôte, G. Szamel, and G. Tarjus for discussions. D.R.R. and K.M. acknowledge support from the NSF (NSF CHE-0134969). G.B. is partially supported by EU contract HPRN-CT-2002-00307 (DYGLAGEMEM). K.M. would like to thank J. D. Eaves for his help on the development of efficient numerical codes.

---

[1] E. Donth, *The glass transition* (Springer, Berlin, 2001).  
 [2] P. G. Debenedetti, F. H. Stillinger, *Nature* **410**, 259 (2001).  
 [3] K. Binder and W. Kob, *Glassy materials and disordered solids* (World Scientific, Singapore, 2005).  
 [4] M. D. Ediger, *Annu. Rev. Phys. Chem.* **51**, 99 (2000).  
 [5] H. Sillescu, *J. Non-Cryst. Solids* **243**, 81 (1999).  
 [6] R. Richert, *J. Phys.: Condens. Matter* **14**, R703 2002 .  
 [7] S. C. Glotzer, *J. Non-Cryst. Solids* **274** 342 (2000).  
 [8] H. C. Andersen, *Proc. Natl. Acad. Sci.* **102**, 6686 (2005).  
 [9] X. Y. Xia and P. G. Wolynes, *Proc. Natl. Acad. Sci.* **97**, 2990 (2000).  
 [10] P. Viot, G. Tarjus, D. Kivelson, *J. Chem. Phys.* **112**, 10368 (2000).  
 [11] J. Jäckle and S. Eisinger, *Z. Phys. B: Condens. Matter* **84**, 115 (1991).  
 [12] G. H. Fredrickson and H. C. Andersen, *Phys. Rev. Lett.* **53**, 1244 (1984); *J. Chem. Phys.* **83**, 958 (1984).  
 [13] S. Butler and P. Harrowell, *J. Chem. Phys.* **95**, 4454 (1991); **95**, 4466 (1991); P. Harrowell, *Phys. Rev. E* **48**, 4359 (1993); M. Foley and P. Harrowell, *J. Chem. Phys.* **98**, 5069 (1993).  
 [14] J. P. Garrahan, D. Chandler, *Phys. Rev. Lett.* **89**, 035704 (2002).  
 [15] S. Whitelam, L. Berthier, J. P. Garrahan, *Phys. Rev. Lett.* **92**, 185705 (2004).  
 [16] G. Biroli and J.-P. Bouchaud, *Europhys. Lett.* **67**, 21 (2004).  
 [17] B. Doliwa and A. Heuer, *Phys. Rev. E* **61**, 6898 (2000).  
 [18] M. M. Hurley and P. Harrowell, *Phys. Rev. E* **52**, 1694 (1995); D. N. Perera and P. Harrowell, *J. Chem. Phys.* **111**, 5441 (1999).  
 [19] R. Yamamoto and A. Onuki, *Phys. Rev. Lett.* **81**, 4915 (1998).  
 [20] Y. Hiwatari and T. Muranaka, *J. Non-Cryst. Solids* **235-237**, 19 (1998).  
 [21] U. Tracht, M. Wilhelm, A. Heuer, H. Feng, K. Schmidt-Rohr, and H. W. Spiess, *Phys. Rev. Lett.* **81**, 2727 (1998).  
 [22] E. Weeks, J.C. Crocker, A.C. Levitt, A. Schofield, and D.A. Weitz, *Science* **287**, 627 (2000).  
 [23] E. Vidal-Russell, N. E. Israeloff, *Nature* **408**, 695 (2000).  
 [24] S. A. Reinsberg, X. H. Qiu, M. Wilhelm, H. W. Spiess,

and M. D. Ediger, *J. Chem. Phys.* **114**, 7299 (2001).

[25] X. H. Qiu and M. D. Ediger, *J. Phys. Chem. B* **107**, 459 (2003).

[26] E. Hempel, G. Hempel, A. Hensel, C. Schick, and E. Donth, *J. Phys. Chem. B* **104**, 2460 (2000).

[27] S. Franz, G. Parisi, *J. Phys.: Condens. Matter* **12**, 6335 (2000).

[28] G. Parisi, *J. Phys. Chem. B* **103**, 4128 (1999).

[29] S. Franz, C. Donati, G. Parisi, and S. C. Glotzer, *Phil. Mag. B*, **79**, 1827, (1999); C. Donati, S. Franz, S. C. Glotzer, and G. Parisi, *J. Non-Cryst. Solids* **307**, 215 (2002).

[30] C. Bennemann, C. Donati, J. Baschnagel, S. C. Glotzer, *Nature* **399**, 246 (1999).

[31] N. Laćević, F. W. Starr, T. B. Schroder, and S. C. Glotzer, *J. Chem. Phys.* **119**, 7372 (2003).

[32] L. Berthier, *Phys. Rev. E* **69**, 020201 (2004).

[33] C. Toninelli, M. Wyart, G. Biroli, L. Berthier, J.-P. Bouchaud, *Phys. Rev. E* **71**, 041505 (2005).

[34] P. Mayer, H. Bissig, L. Berthier, L. Cipelletti, J. P. Garrahan, P. Sollich, and V. Trappe, *Phys. Rev. Lett.* **93**, 115701 (2004).

[35] O. Dauchot, G. Marty and G. Biroli, *Phys. Rev. Lett.* **95**, 265701, (2005).

[36] L. Berthier, G. Biroli, J.-P. Bouchaud, L. Cipelletti, D. El Masri, D. L'Hôte, F. Ladieu, and M. Pierno, *Science* **310**, 1797 (2005).

[37] L. Berthier, G. Biroli, J.-P. Bouchaud, W. Kob, K. Miyazaki, D. R. Reichman, companion paper.

[38] J.-P. Bouchaud, L. F. Cugliandolo, J. Kurchan and M. Mézard, *Physica A* **226**, 243 (1996).

[39] W. Götze, *J. Phys. Cond. Matt.* **11**, A1 (1999). W. Götze and L. Sjögren, *Rep. Prog. Phys.* **55**, 241 (1992).

[40] F. Ritort and P. Sollich, *Adv. Phys.* **52**, 219 (2003).

[41] R. M. Ernst, S. R. Nagel, and G. S. Grest, *Phys. Rev. B* **43**, 8070, (1991).

[42] K. Binder and A. P. Young, *Rev. Mod. Phys.* **58**, 801 (1986).

[43] S. F. Edwards and P. W. Anderson, *J. Phys. F : Metal Phys.* **5** 965 (1975).

[44] J.-P. Bouchaud, G. Biroli, *Phys. Rev. B* **72** 064204 (2005).

[45] This was recently shown rigorously for a large class of glassy dynamics in A. Montanari, G. Semerjian, cond-mat/0603018, and suggested in full generality by the bound derived in [36].

[46] J. P. Hansen, I. R. Mc Donald, *Theory of simple liquids* (Elsevier, Amsterdam, 1986).

[47] T. R. Kirkpatrick and D. Thirumalai, *Phys. Rev. A* **37**, 4439 (1988).

[48] G. Biroli, J.-P. Bouchaud, K. Miyazaki, and D. R. Reichman, preprint cond-mat/0605733.

[49] D. Chandler, J. P. Garrahan, R. L. Jack, L. Maibaum and A. C. Pan, preprint cond-mat/0605084.

[50] L. Cipelletti and L. Ramos, *J. Phys. : Condens. Matter* **17**, R253 (2005).

[51] M. Allen and D. Tildesley, *Computer Simulation of Liquids* (Oxford University Press, Oxford, 1987).

[52] B. Doliwa and A. Heuer, *Phys. Rev. E* **61**, 6898 (2000).

[53] P. N. Pusey, W. van Megen, *Nature* **320**, 340 (1986).

[54] J. L. Lebowitz, J. K. Percus, L. Verlet, *Phys. Rev.* **153**, 250 (1967).

[55] M. D. Ediger, *J. Non-Cryst. Solids* **235-237**, 10 (1998).

[56] L. D. Landau and E. M. Lifshitz, *Statistical Physics, Course of Theoretical Physics, Vol. 5, Pt. 1* (Pergamon, New York, 1980).

[57] G. Tarjus, D. Kivelson, S. Mossa, C. Alba-Simionescu, *J. Chem. Phys.* **120**, 6135 (2004).

[58] J. Zinn Justin, *Quantum field theory and critical phenomena* (Oxford University Press, Oxford, 2002).

[59] D. S. Dean, *J. Phys. A* **29**, L613 (1996).

[60] K. Kawasaki, *Physica A* **208**, 35 (1994).

[61] A. Andreanov, G. Biroli, and A. Lefèvre, *J. Stat. Mech.* P07008 (2006).

[62] S. P. Das, *Rev. Mod. Phys.* **76**, 785 (2004).

[63] J. Cardy, *Scaling and Renormalization in Statistical Physics* (Cambridge University Press, Cambridge, 1996).

[64] C. De Dominicis and P. Martin, *J. Math. Phys.* **5**, 14 and 31 (1964).

[65] J.-P. Blaizot, G. Ripka, *Quantum Theory of Finite Systems* (Editions Phenix, Kiev, 1998).

[66] K. Miyazaki and D. R. Reichman, *J. Phys. A: Math. Gen.* **38**, L343 (2005).

[67] T. Gleim, W. Kob, and K. Binder, *Phys. Rev. Lett.* **81**, 004404 (1998).

[68] G. Szamel, and E. Flenner, *Europhys. Lett.* **67**, 779 (2004).

[69] W. Kob and H. C. Andersen, *Phys. Rev. Lett.* **73**, 1376 (1994); *Phys. Rev. E* **53**, 4134 (1995); *Phys. Rev. E* **51**, 4626 (1995).

[70] B. W. H. van Beest, G. J. Kramer, and R. A. van Santen, *Phys. Rev. Lett.* **64**, 1955 (1990).

[71] S. N. Taraskin and S. R. Elliott, *Europhys. Lett.* **39**, 37 (1997); M. Benoit, S. Ispas, P. Jund, and R. Jullien, *Eur. Phys. J. B* **13**, 631 (2000); J. Horbach and W. Kob, *Phys. Rev. B* **60**, 3169 (1999); *Phys. Rev. E* **64**, 041503 (2001).

[72] L. Berthier and W. Kob, in preparation.

[73] M. Vogel and S. C. Glotzer, *Phys. Rev. Lett.* **92**, 255901 (2004); *Phys. Rev. E* **70**, 061504 (2004).

[74] L. Berthier, *Phys. Rev. Lett.* **91**, 055701 (2003).

[75] G. Szamel and E. Flenner, *Phys. Rev. E* **74**, 021507 (2006).

[76] E. Flenner, G. Szamel, cond-mat/0608398.

[77] J. P. Garrahan and D. Chandler, *Proc. Natl. Acad. Sci.* **100**, 9710 (2003).

[78] A. Widmer-Cooper, P. Harrowell, and H. Fynnewever, *Phys. Rev. Lett.* **93**, 135701 (2004); A. Widmer-Cooper and P. Harrowell, *Phys. Rev. Lett.* **96**, 185701 (2006).

[79] A similar expression could be obtained when  $C_o(\mathbf{r}, t)$  is computed using a time average instead of a space average; the resulting variance would now measure the temporal correlation of the temporal correlation.

[80] Note that for the energy we use the notation  $E(t=0) = \frac{1}{N} \int d\mathbf{x} e(\mathbf{x}, t=0)$ . Therefore,  $e$  is an energy per unit volume.

[81] Note that since the value of the physical fields is fixed by the initial conditions and not changed by loop corrections is often more useful and practical to develop the theory in terms of  $\delta\Psi$  so that the average of the fluctuating fields is zero by construction.

[82] We restrict here to the case  $t = \tau_\alpha$ ; the full dependence of these different correlators with time will be discussed in the companion paper, Ref. [37].